International Journal of Earth Sciences (2023) 112:999–1022
https://doi.org/10.1007/s00531-022-02275-1

ORIGINAL PAPER

No sediment transport across the Tethys ocean during the latest Cretaceous: detrital zircon record from the Pontides and the Anatolide–Tauride Block

Aral I. Okay[1] · **Andrew R. C. Kylander-Clark**[2]

Received: 18 July 2022 / Accepted: 18 November 2022 / Published online: 7 December 2022

Abstract
We report detrital zircon ages from the Upper Cretaceous (Campanian–Maastrichtian) turbiditic sandstones from the Pontides and the Anatolide–Tauride Block, which were located on opposite margins of the Tethys ocean during most of the Paleozoic and Mesozoic. The large data set includes both published and new detrital zircon ages from the Upper Cretaceous Pontide sandstones (2730 zircon ages from 26 samples) and new detrital zircon ages from the uppermost Cretaceous Bornova Flysch of the Anatolide–Tauride Block (378 ages from five samples). Phanerozoic detrital zircons from the Upper Cretaceous sandstones of the Pontides are predominantly Late Cretaceous (56%) followed by Carboniferous (7.9%), Devonian (5.3%), Jurassic (3.1%) and Triassic (2.9%). In contrast, there are no Cretaceous and Jurassic detrital zircons in the uppermost Cretaceous Bornova Flysch, and the Phanerozoic detrital zircon populations are mainly Carboniferous (41.3%), Triassic (7.1%), Permian (6.9%) and Devonian (5.3%). The absence of Cretaceous and Jurassic zircons in the Bornova Flysch shows that there was no sediment transport between the Pontides and the Anatolide–Tauride Block during the latest Cretaceous (75–70 Ma); it also shows that the latest Cretaceous – Paleocene deformation of the Bornova Flysch Zone predates the collision between the Pontides and the Anatolide–Tauride Block, and is associated with ophiolite obduction. The dominance of Carboniferous detrital zircons in the Bornova Flysch Zone underlines that Carboniferous magmatic activity in the Anatolide–Tauride Block, and hence on the northern margin of Gondwana, was more significant than hitherto recognized.

Keywords Detrital zircons · Late Cretaceous · Pontides · Bornova Flysch Zone · Anatolide–Tauride Block · Carboniferous

Introduction

The Late Cretaceous was tectonically an active period in the Eastern Mediterranean–Aegean region with multiple episodes of metamorphism, deformation and magmatism related to subduction, ophiolite obduction and inception of continental collision (e.g., Robertson et al. 2013; Okay and Nikishin 2015; van Hinsbergen et al. 2020). This has led to a complex geology with large number of tectonic units, the affinity and the time of juxtaposition of these units are often controversial. Detrital zircon geochronology has the potential to constrain the origin of the tectonic units and the time of their amalgamation. It also frequently provides information on magmatic events, the record of which could be concealed beneath young sedimentary and tectonic cover or removed by erosion (e.g., Gehrels 2014; Ustaömer et al. 2013; Akdoğan et al. 2017). Here, we report detrital zircon ages and sandstone petrography from Upper Cretaceous turbidites from the Pontides and from the Anatolide–Tauride Block, which were separated by a Tethyan ocean during the Paleozoic and Mesozoic. The results show that, in contrast to that implied in some recent paleogeographic reconstructions (Moix et al. 2008; Robertson et al. 2013; Barrier et al. 2018), there was no sediment transport between the Pontides and the Anatolide–Tauride Block during the Late Cretaceous (75–70 Ma). On a broader scale this shows that the Tethyan ocean provided an effective barrier between Gondwana and Eurasia during the latest Cretaceous, as also suggested by

✉ Aral I. Okay
okay@itu.edu.tr

Andrew R. C. Kylander-Clark
kylander@geol.ucsb.edu

1 Eurasia Institute of Earth Sciences, İstanbul Technical University (İTÜ), Ayazağa, Istanbul, Turkey

2 Department of Earth Sciences, University of California, Santa Barbara, CA, USA

some early paleogeographic reconstructions (e.g., Robertson and Dixon 1984; Dercourt et al. 1986). Furthermore, the detrital zircon ages from the Anatolide–Tauride Block show a major Carboniferous peak, reinforcing recent data for the presence of Carboniferous magmatism on the northwestern margin of Gondwana.

Geological setting

During most of the Paleozoic and Mesozoic, the Pontides formed part of the active continental margin of Laurasia facing the İzmir–Ankara–Erzincan ocean in the south. The trace of this ocean is represented today by the İzmir–Ankara–Erzincan suture (Fig. 1, e.g., Okay and Tüysüz 1999; Robertson et al. 2013). The Pontides became separated from the bulk of Laurasia with the Late Cretaceous opening of the Black Sea as a back-arc basin (e.g., Görür 1988; Okay et al 1994). On the other hand, the Anatolide–Tauride Block was located south of the İzmir–Ankara–Erzincan ocean and formed a passive margin in the Mesozoic. During the Neoproterozoic and Paleozoic, the Anatolide–Tauride Block was part of Gondwana;

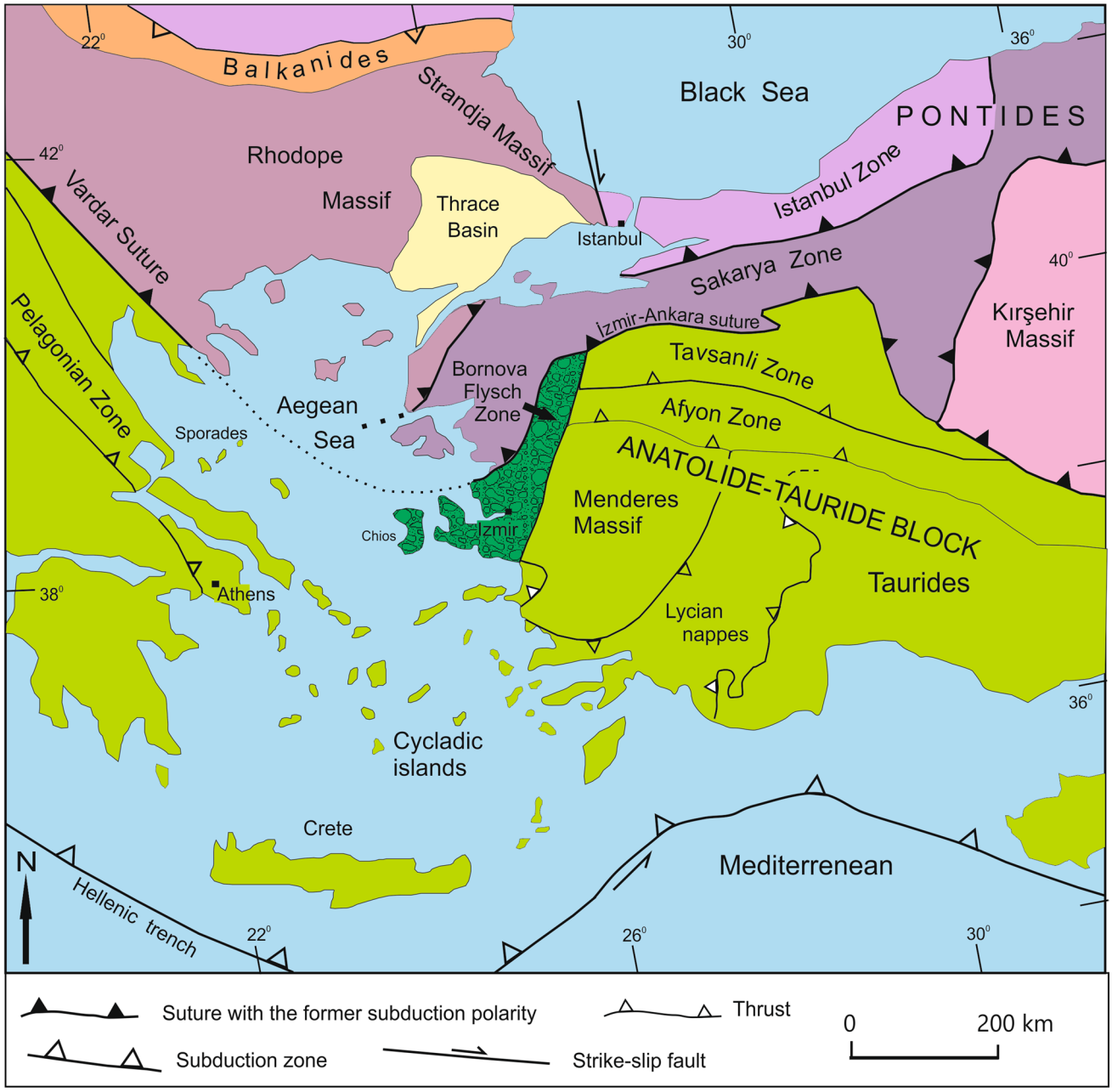

Fig. 1 Tectonic map of the Aegean region

it rifted off from Gondwana with the opening of the Bitlis–Zagros ocean in the Permo-Triassic; the present Eastern Mediterranean represents a relic of this ocean (e.g., Şengör and Yılmaz 1981). Below, we summarize the geology of the Pontides and the Anatolide–Tauride Block with special emphasis on major pre-Cenozoic magmatic episodes, which provide a source for detrital zircons.

Pontides

The Pontides consist of three Gondwana-derived units, the Istanbul Zone, the Sakarya Zone and the Strandja Massif (Fig. 1), which were welded to Laurasia at different periods (Okay and Tüysüz 1999). Upper Cretaceous volcanic and volcaniclastic sequences extend throughout the Sakarya, İstanbul zones and the Strandja Massif (Fig. 2) and provide an upper age limit for their amalgamation.

The Istanbul Zone has a thick, well-developed, continuous Ordovician to Carboniferous sedimentary sequence, which lies unconformably over a late Neoproterozoic basement of granites (580–560 Ma) and metamorphic rocks (Fig. 3, Dean et al. 2000; Chen et al. 2002; Ustaömer et al. 2005; Özgül 2012). The Paleozoic rocks of the Istanbul Zone were deformed during the Carboniferous orogeny and

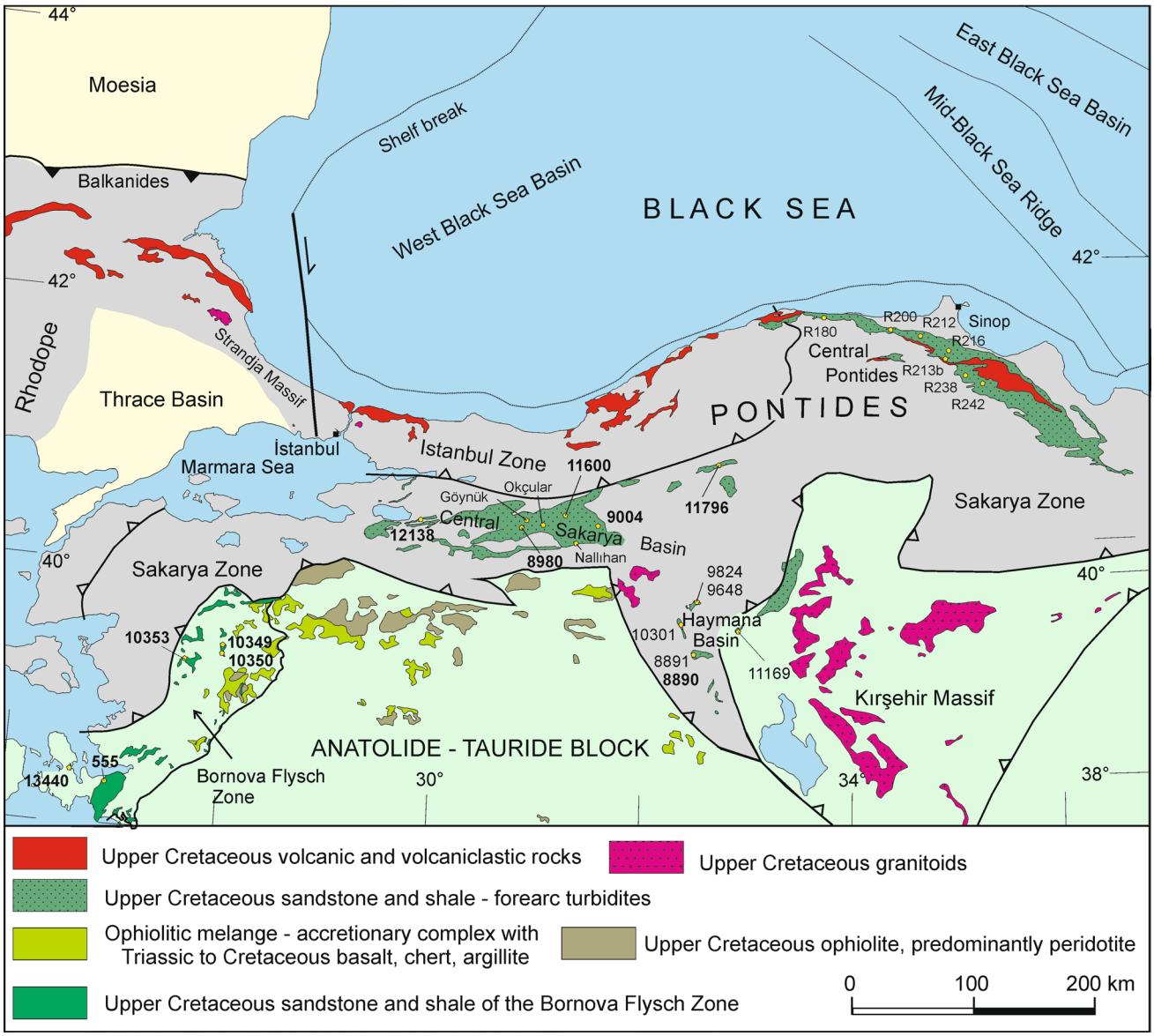

Fig. 2 Geological map of northwestern and central Anatolia showing the outcrops of the Upper Cretaceous magmatic and sedimentary rocks, and sample localities. The base map is from Konak et al. (2016). The bold numbers represent new samples reported in this study. Nallıhan, Okçular and Göynük localities refer to samples from stratigraphic sections sampled by Mueller et al. (2022)

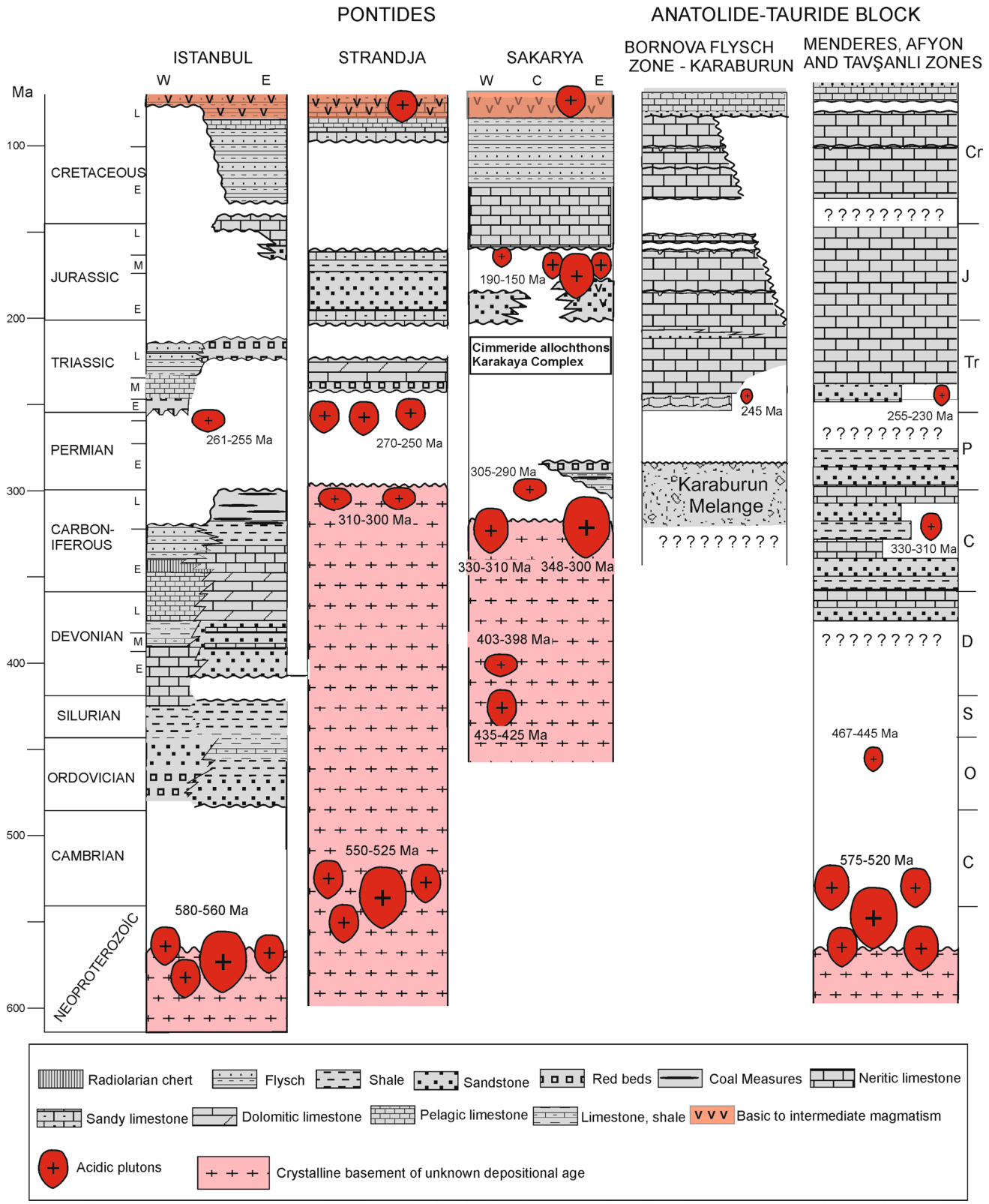

Fig. 3 Generalized stratigraphic columns for the Pontides and the Anatolide–Tauride Block with special emphasis on granitic magmatism. For sources see the text

intruded by Permian (261–255 Ma) granites (Aysal et al. 2018). A sedimentary Upper Permian–Triassic sequence lies unconformably over the Paleozoic series. Upper Jurassic – Lower Cretaceous series is only preserved in the eastern part of the Istanbul Zone and consists of shallow marine limestones and sandstones (Okay et al. 2018). During the Late Cretaceous, a magmatic arc formed, which can be followed all along the southern margin of the Black Sea (Fig. 2). The pre-Cenozoic magmatic rocks in the Istanbul Zone are of late Neoproterozoic (580–560 Ma), Permian (261–255 Ma) and Late Cretaceous ages.

The Strandja Massif has also a late Neoproterozoic to Cambrian (550–525 Ma) basement of granitic and metamorphic rocks overlain by a poorly dated Paleozoic sedimentary series (Yılmaz Şahin et al. 2014; Yılmaz et al. 2021). It was deformed and metamorphosed during the Carboniferous Variscan orogeny and was subsequently intruded by voluminous Upper Carboniferous and Permian (319–250 Ma) granites (Fig. 3; Sunal et al. 2006; Aysal et al. 2018; Akgündüz et al. 2021; Sałacinska et al. 2022). More recently Middle Triassic (245–237 Ma) granites are also described from the Bulgarian sector of the Strandja Massif (Bonev et al. 2022). The Variscan crystalline basement and the Permo-Carboniferous granites are unconformably overlain by a Triassic–Jurassic sedimentary sequence. Regional metamorphism and deformation during the latest Jurassic have affected both the Variscan basement and its Mesozoic cover (Okay et al. 2001; Sunal et al. 2011). The metamorphic rocks are unconformably overlain by early Upper Cretaceous (Cenomanian) sandstones, which pass up into a Santonian to Campanian volcanic and volcaniclastic rocks. The magmatic rocks in the Strandja Massif are of late Neoproterozoic–Cambrian (550–525 Ma), Late Carboniferous–Middle Triassic (319–237 Ma) and Late Cretaceous ages.

The Sakarya Zone has a complex, heterogeneous pre-Jurassic basement consisting mainly of three tectonic units (Fig. 3): a) A Variscan basement of high-grade metamorphic rocks with late Neoproterozoic to Silurian (435–425 Ma) metagranites (Topuz et al. 2020; Karslı et al. 2020; Dokuz et al. 2022). The metamorphism was Early Carboniferous (340–330 Ma) in age and the metamorphic rocks are intruded by Carboniferous–Early Permian (348–290 Ma) granites (Topuz et al. 2010, 2020; Kaygusuz et al. 2012, 2016; Ustaömer et al. 2012). b) Permian–Triassic subduction–accretion complexes consisting of metabasite, phyllite and marble, and highly deformed siliciclastic turbidites, called as the Karakaya Complex (Okay and Göncüoğlu 2004). c) Early Devonian (403–398) granites (Aysal et al. 2012; Topuz et al. 2020; Karslı et al. 2020).

The basement of the Sakarya Zone is stratigraphically overlain by a Jurassic–Cretaceous sedimentary and volcanic sequence (Fig. 3). The Jurassic is characterized by arc-related volcanic rocks and intrusive granites (190–150 Ma), which outcrop widely across the Sakarya Zone (Okay et al. 2014, 2018; Eyuboglu et al. 2016; Gücer et al. 2016; Çimen et al. 2017; Liu et al. 2021; Sunal et al. 2022). These are overlain by Upper Jurassic–Lower Cretaceous limestones, which pass up into the Upper Cretaceous volcanic and volcaniclastic rocks. The magmatic rocks in the Sakarya Zone are mainly of Silurian (435–425 Ma), Devonian (403–398 Ma), Carboniferous–Early Permian (348–290 Ma), Jurassic (190–150 Ma) and Late Cretaceous ages.

As discussed above, the Pontides were affected by widespread magmatism throughout the late Neoproterozoic and Phanerozoic, which is a consequence of their location in an active margin. A proxy for the intensity and duration of magmatism throughout this long period is the bedrock magmatic ages. The bedrock ages also enable an objective correlation with the detrital zircon record. We compiled published pre-Cenozoic zircon bedrock ages from magmatic rocks from the Pontides, which are given in Table S1 and shown in Fig. 4a. The data set includes 220 zircon ages from the magmatic rocks, mostly granites. The most dominant zircon age group is Late Cretaceous (77 Ma), followed by Jurassic (ca. 177 Ma), Carboniferous (340–302 Ma), Devonian (405–397 Ma) and Cambrian–Neoproterozoic (580–530 Ma). Ordovician magmatic rocks are very rare and Triassic ones are represented by small granitic bodies in the Strandja Massif (Fig. 4a).

The Anatolide–Tauride Block

Unlike the Pontides, the Anatolide–Tauride Block formed a single plate during the Mesozoic and its tectonic subdivision is largely a consequence of the Late Cretaceous and younger Alpine tectonics (Okay 2008). The Tavşanlı Zone in the north represents the northern subducted margin of the Anatolide–Tauride Block with the high pressure – low temperature (HP/LT) metamorphism dated as Late Cretaceous (ca. 80 Ma, Sherlock et al. 1999). The Afyon Zone was metamorphosed at high-pressure greenschist facies at the end of Cretaceous (ca. 66 Ma, Pourteau et al. 2013; Özdamar et al. 2013). The Cycladic Complex underwent HP/LT metamorphism during the Early Eocene (ca. 52 Ma, e.g., Bröcker and Enders 2001; Lagos et al. 2007; Çetinkaplan et al. 2020), and the Menderes Massif a Barrovian-type metamorphism during the Middle–Late Eocene (43–35 Ma, Hetzel and Reischmann 1996; Schmidt et al. 2015). The Bornova Flysch Zone forms a northeast trending belt between the Alpine metamorphic zones and the İzmir–Ankara–Erzincan suture (Fig. 1, Okay and Siyako 1993). It consists of deformed Upper Cretaceous to Paleocene olistostromes (Okay et al. 2012). The Lycian Nappes and the Taurides are made up predominantly of Paleozoic and Mesozoic sedimentary sequences (e.g., Özgül 1976; Gutnic et al. 1979).

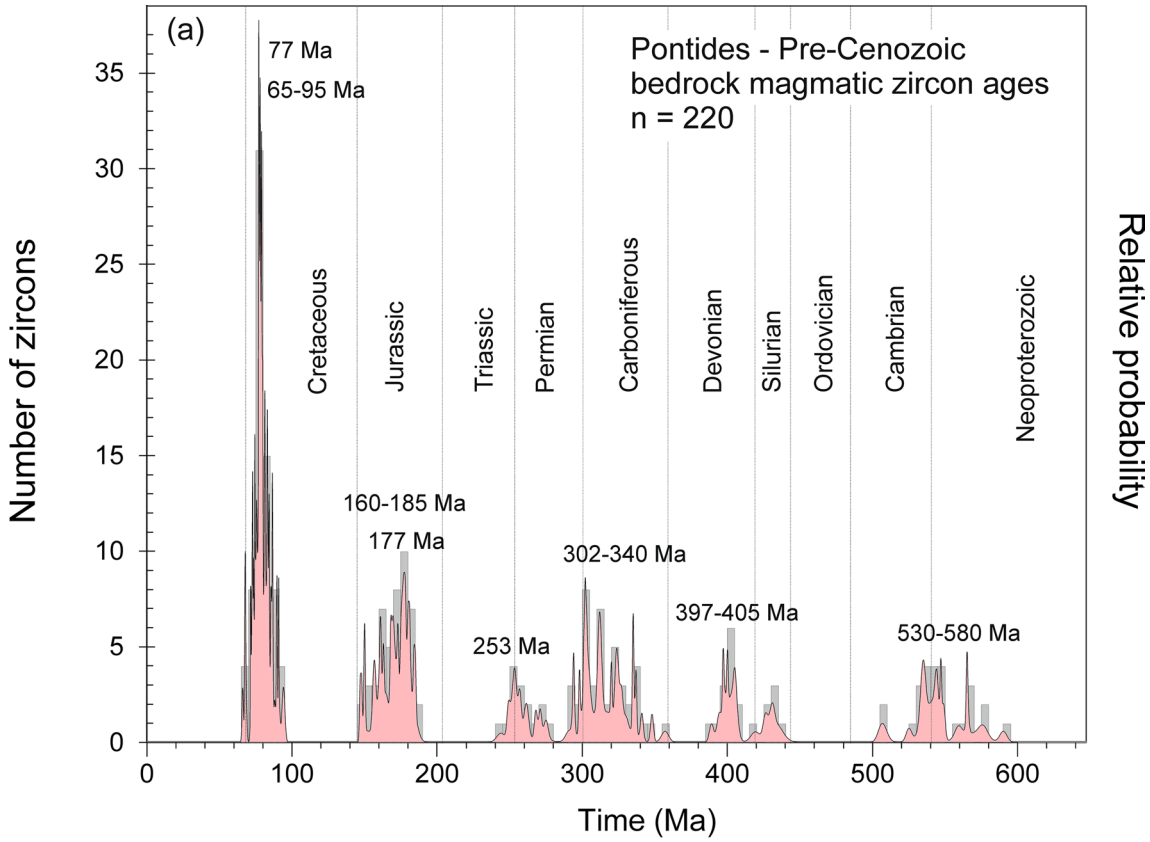
(a)
Pontides - Pre-Cenozoic
bedrock magmatic zircon ages
n = 220
77 Ma
65-95 Ma
160-185 Ma
177 Ma
253 Ma
302-340 Ma
397-405 Ma
530-580 Ma
Cretaceous
Jurassic
Triassic
Permian
Carboniferous
Devonian
Silurian
Ordovician
Cambrian
Neoproterozoic
Number of zircons
Relative probability
Time (Ma)
0
5
10
15
20
25
30
35
0
100
200
300
400
500
600

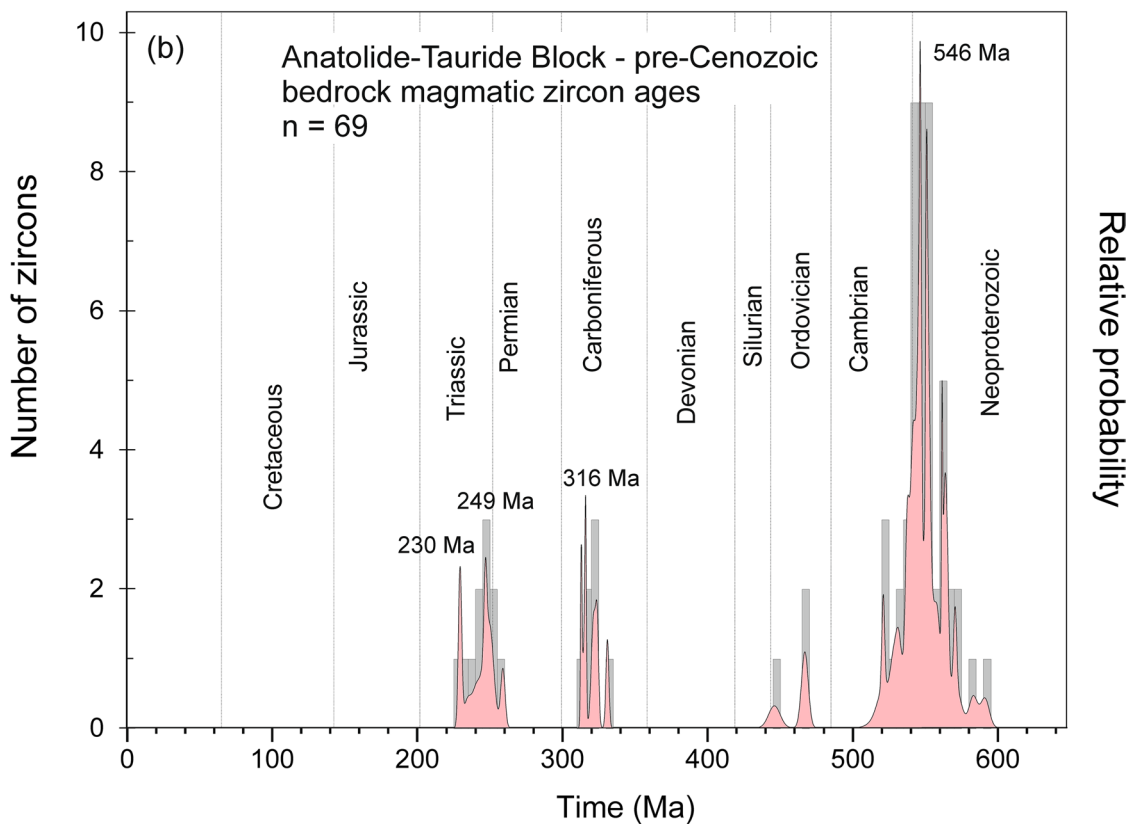
(b)
Anatolide-Tauride Block - pre-Cenozoic
bedrock magmatic zircon ages
n = 69
546 Ma
316 Ma
249 Ma
230 Ma
Cretaceous
Jurassic
Triassic
Permian
Carboniferous
Devonian
Silurian
Ordovician
Cambrian
Neoproterozoic
Number of zircons
Relative probability
Time (Ma)
0
2
4
6
8
10
0
100
200
300
400
500
600

◂**Fig. 4** Zircon ages from pre-Cenozoic magmatic bedrocks from the Pontides **a** and the Anatolide–Tauride Block. **b** Note the difference in scale between **a** and **b**, which is a reflection of the dominance of magmatic rocks in the Pontides compared to the Anatolide–Tauride Block. The bin widths are 5 my. For sources of data see Table S1

The Anatolide–Tauride Block has also an Early Cambrian—Neoproterozoic (575–520 Ma) granitic and metamorphic basement well exposed in the core the Menderes Massif (Fig. 5; Loos and Reischmann 1999; Gessner et al. 2004; Candan et al. 2011; Koralay et al. 2011; Zlatkin et al. 2013;). This Panafrican basement is overlain by a predominantly sedimentary Paleozoic and Mesozoic series. Phanerozoic magmatic rocks are rare in the Anatolide–Tauride Block, and make up less a few percent the sequence, which is a result of its position in a passive margin during most of the Paleozoic and Mesozoic. Unlike the Pontides, there are no Jurassic or Cretaceous granitic rocks in the western and central parts of the Anatolide–Tauride Block. Two small outcrops of Ordovician (467–445 Ma) and a larger outcrop of Carboniferous (330–310 Ma) metagranites are described from the Tavşanlı and Afyon zones, respectively (Fig. 5; Okay et al. 2008; Özbey et al. 2013; Candan et al. 2016; Ustaömer et al. 2020). Small Early–Middle Triassic (255–220 Ma) metagranites are reported from the Menderes Massif (Koralay et al. 2001, 2011; Ustaömer et al. 2016), from the Afyon Zone (Akal et al. 2012; Özdamar et al. 2013; Ustaömer et al. 2016) and from the Bornova Flysch Zone (Erkül et al. 2008; Akal et al. 2011, Ustaömer et al. 2016).

We also compiled pre-Cenozoic bedrock magmatic zircon ages from the Anatolide–Tauride Block (Table S1, Fig. 4b). The data set includes 69 ages from magmatic bodies (mostly granites) from the western and central parts of the Anatolide–Tauride Block. In stark contrast to the Pontides, there are no Cretaceous or Jurassic magmatic rocks in the western and central parts of the Anatolide–Tauride Block; minor Upper Cretaceous granites are restricted to the Eastern Taurides in the eastern Anatolia (e.g., Robertson et al. 2021). The magmatic zircons in the Anatolide–Tauride Block are predominantly Neoproterozoic–Cambrian (ca. 546 Ma), Carboniferous (ca. 316 Ma) and Triassic (ca. 249 Ma) in age (Fig. 4b). The dominance of Neoproterozoic–Cambrian ages reflects the large outcrops of Pan-African metagranites at the core of the Menderes Massif (Fig. 5).

Methods

Rock samples were collected in outcrop from the Pontides and the Bornova Flysch Zone of the Anatolide–Tauride Block. The locations of the samples in UTM coordinates are given in Table S2. The samples were processed in the Eurasia Institute of Earth Sciences of the Istanbul Technical University. Mineral separation for zircon dating was done using classical techniques involving crushing, sieving, magnetic and heavy liquid separation. The zircons were picked under a binocular microscope and mounted in epoxy and were polished to nearly half width of the grains. Internal structures of the mounted zircons were imaged by means of cathodoluminescence (CL) in the Hacettepe University (Ankara) by ZeissEvo-50SEM. The CL images of the analyzed zircons are given in the Supplementary Figs. S1 and S2. Zircons were analyzed using laser ablation inductively coupled plasma mass spectrometry (LA-ICPMS) at the University of California, Santa Barbara. For the details of the method employed, see Kylander-Clark et al. (2013). Long-term reproducibility in secondary reference materials is < 2% and, as such, should be used when comparing ages obtained within this analytical session to ages elsewhere. The U-Pb analytical data are given in the Supplementary Table S3.

Detrital zircon data from the Upper Cretaceous sandstones of the Pontides

During the Late Cretaceous the northern parts of the Pontides formed a magmatic arc, represented mainly by volcanic and volcaniclastic rocks of Santonian to Campanian ages (e.g., Okay and Nikishin 2015). The volcanic rocks pass southward to coeval siliciclastic turbidites deposited in forearc basins (Fig. 2; Görür et al. 1998; Ocakoğlu et al. 2019; Mueller et al. 2022). The forearc basins shallow during the Maastrichtian and the turbidites pass up into sandstones and limestones. Arc volcanism also waned towards the end of the Cretaceous and was replaced by carbonate deposition. Samples for detrital zircon study come from the Upper Cretaceous forearc turbidites from three areas in the Pontides (Fig. 2). The first one is the Central Sakarya Basin, where there is a well-preserved Jurassic to Paleocene sequence (e.g., Saner 1980; Ocakoğlu et al. 2019). From this region, we report 476 new detrital zircon ages from five samples of which 364 are concordant at 90–110%; the new data augment detrital zircon ages from eight samples reported by Mueller et al. (2022). The second area is the Haymana basin, which shows a similar stratigraphy as the Central Sakarya Basin (Ünalan et al. 1976; Okay and Altıner 2016). The detrital zircon data from the Upper Cretaceous sandstones from the Haymana Basin are largely taken from Okay et al. (2019, 2020) with one new sample (8890) from which we report 95 concordant ages out of 116 analyses. The third area is in the Central Pontides, where we use detrital zircon ages from the seven Upper Cretaceous sandstones reported by Akdoğan et al. (2019). The depositional ages of the samples, constrained by regional biostratigraphy, are Campanian–Maastrichtian; the youngest significant detrital zircons indicate that most samples are late Campanian

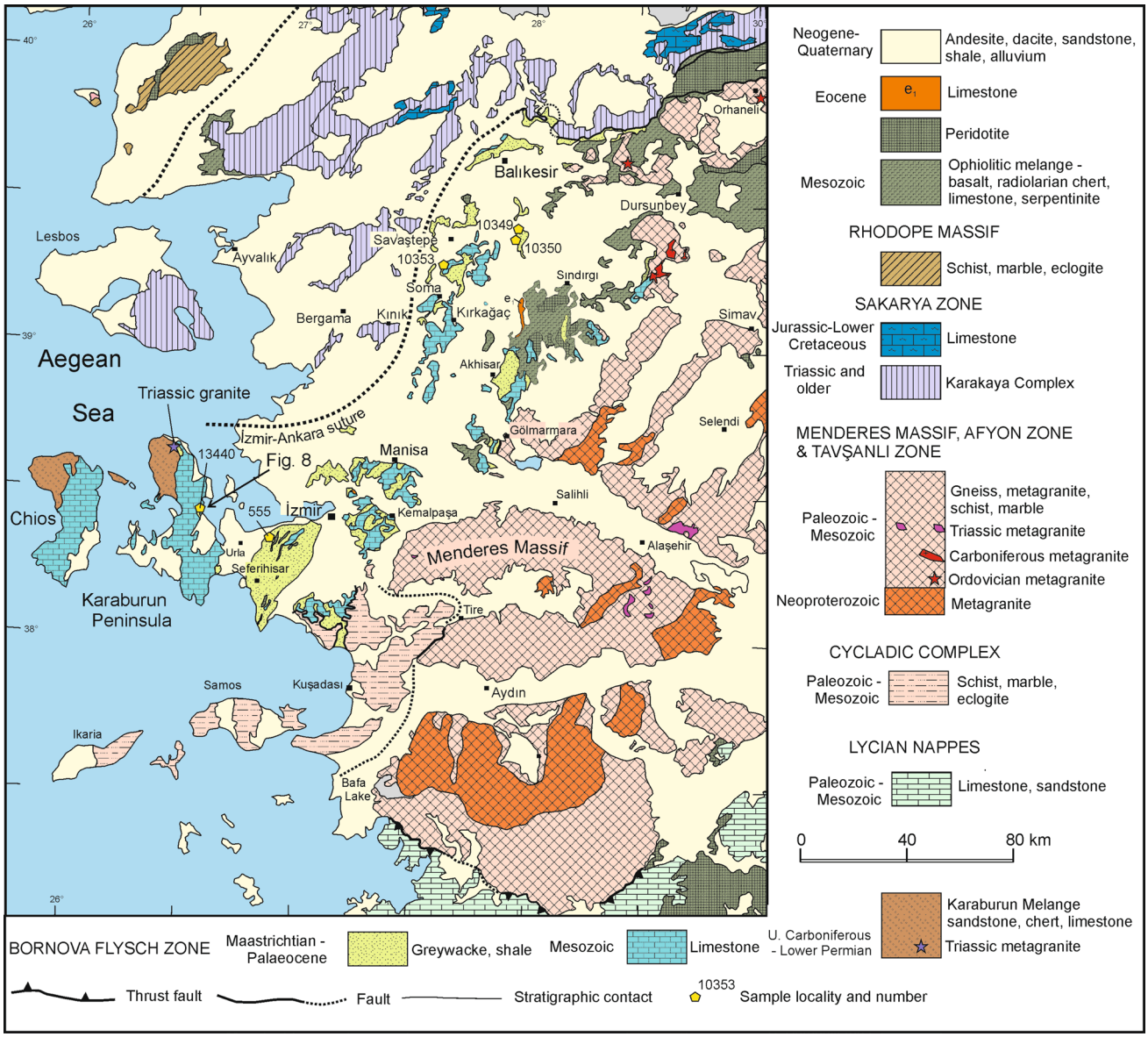

Fig. 5 Geological map of the Bornova Flysch Zone and surrounding tectonic units (modified from Okay et al. 2012)

– Maastrichtian (75–70 Ma) in age (Table 1). The CL images of the analyzed zircons from six samples are given in Figure S1; the majority of zircons are euhedral and show igneous zoning indicating a magmatic origin.

The age spectrum based on 2730 concordant zircon ages from 26 Upper Cretaceous sandstone samples is shown in Fig. 6a. As expected, from the forearc setting of the sandstones, the age spectrum is dominated by the Late Cretaceous zircons (68–105 Ma), which make up nearly half (49%, 1325 zircons) of the total zircon population. The peak Late Cretaceous ages in individual samples are predominantly 71–74 Ma supporting the late Campanian—early Maastrichtian depositional ages of the sandstones (Fig. 7). Other major Phanerozoic age groups are Carboniferous (216 zircons, 7.9%), Devonian (145 zircons, 5.3%), Jurassic (85 zircons, 3.1%), Triassic (80 zircons, 2.9%) and Permian (77 zircons, 2.8%). Some age groups have well-defined peaks such as at 166 Ma (Middle Jurassic), 300 Ma (Carboniferous–Permian boundary), 325 Ma (Carboniferous) and 390 Ma (Devonian); other age groups show a more homogeneous age distribution as the case for the Triassic (210–250 Ma) and Neoproterozoic zircons (560–650 Ma, 313 zircons, 11.5%). Mesoproterozoic to Archean zircons (177 zircons) make up 6.5% of the whole zircon population (Fig. 6a).

There is considerable heterogeneity in detrital zircon ages among the individual Upper Cretaceous sandstone samples (Fig. 7). Although the Late Cretaceous zircons are overall

Table 1 List of the samples from the Upper Cretaceous sandstones from the Pontides and the Bornova Flysch Zone

	Sample no	Locality	Sub-basin	Rock type	Depositional age	Youngest significant age	No. of concordant zircon ages	Reference
Samples from the Upper Cretaceous sandstones of the Bornova Flysch Zone								
1	555	Buca		Sandstone	Maastrichtian—Paleocene	222 Ma	103	This study
2	10,349	Bigadiç		Sandstone	Campanian—Maastrichtian	235 Ma	64	This study
3	10,350	Bigadiç		Sandstone	Campanian—Maastrichtian	236 Ma	46	This study
4	10,353	Soma		Sandstone	Campanian—Maastrichtian	214 Ma	130	This study
5	13,440	Balıklıova, Karaburun	Top of the Karaburun succession	Sandstone	Maastrichtian	239 Ma	35	This study
Samples from the Upper Cretaceous sandstones of the Pontides								
1	8890	Haymana	Haymana Basin (HB)	Sandstone	Campanian	82 Ma	95	This study
2	8891	Haymana	HB	Sandstone	Campanian	75 Ma	61	Okay et al. (2019)
3	9648	Alcı, Ankara	HB	Sandstone	Campanian	73 Ma	51	Okay et al. (2019)
4	9824	Alcı, Ankara	HB	Sandstone	Campanian	75 Ma	83	Okay et al. (2019)
5	10,301	Polatlı	HB	Sandstone	Maastrichtian	72 Ma	103	Okay et al. (2019)
6	11,169	Beynam	HB	Sandstone	Campanian	81 Ma	49	Okay et al. (2022)
7	R180	Sinop	Central Pontides (CP)	Sandstone	Campanian—Maastrichtian	262 Ma	127	Akdoğan et al. (2019)
8	R200	Sinop	CP	Sandstone	Campanian	77 Ma	106	Akdoğan et al. (2019)
9	R212	Sinop	CP	Sandstone	Campanian—Maastrichtian	159 Ma	104	Akdoğan et al. (2019)
10	R213B	Sinop	CP	Sandstone	Campanian	75 Ma	94	Akdoğan et al. (2019)
11	R216A	Sinop	CP	Sandstone	Campanian	73 Ma	52	Akdoğan et al. (2019)
12	R238	Sinop	CP	Sandstone	Campanian—Maastrichtian	95 Ma,		
165 Ma	84	Akdoğan et al. (2019)						
13	R242	Sinop	CP	Sandstone	Campanian—Maastrichtian	104 Ma,		
158 Ma	70	Akdoğan et al. (2019)						
14	11,796	Çerkeş	Central Sakarya Basin (CSB)	Sandstone	Campanian—Maastrichtian	111 Ma	83	This study
15	11,600	Mudurnu	CSB	Sandstone	Campanian	73 Ma	64	This study
16	8980	Göynük	CSB	Sandstone	Maastrichtian	72 Ma	65	This study
17	9004	Seben	CSB	Sandstone	Maastrichtian	72 Ma	76	This study
18	12,138	İznik	CSB	Sandstone	Campanian—Maastrichtian	233 Ma	76	This study
19	17MGB01	Göynük	CSB	Sandstone	Santonian—Campanian	89 Ma	155	Mueller et al. (2022)
20	CC082910	Nallıhan	CSB	Sandstone	Maastrichtian	72 Ma	161	Mueller et al. (2022)
21	18NAL12	Nallıhan	CSB	Sandstone	Maastrichtian	68 Ma	150	Mueller et al. (2022)

Table 1 (continued)

	Sample no	Locality	Sub-basin	Rock type	Depositional age	Youngest significant age	No. of concordant zircon ages	Reference
22	18NAL13	Nallıhan	CSB	Sandstone	Maastrichtian	70 Ma	156	Mueller et al. (2022)
23	18NAL05	Nallıhan	CSB	Sandstone	Campanian	78 Ma	159	Mueller et al. (2022)
24	CC082918	Nallıhan	CSB	Sandstone	Cenomanian—Turonian	95 Ma	165	Mueller et al. (2022)
25	18DMN01	Okçular	CSB	Sandstone	Campanian	85 Ma	180	Mueller et al. (2022)
26	18YP02	Okçular	CSB	Sandstone	Campanian	76 Ma	160	Mueller et al. (2022)

by far the most dominant age group, their percentage various from 0 to 100% among samples from all the three subbasins (Fig. 7). There is also major variation among samples for other age groups, which indicates that other sources besides the Upper Cretaceous volcanic arc were temporally and locally significant.

There is a good correlation between the magmatic bedrock and detrital zircon ages from the Pontides (cf. Figs. 4a and 5a). Late Cretaceous and Middle Jurassic magmatic arcs provide most of the zircons; the Carboniferous and Neoproterozoic zircons can be traced to the basement granites of the Sakarya and Istanbul zones, respectively. One apparent discrepancy is the presence of Triassic detrital zircons in the Upper Cretaceous sandstones compared to the lack of Triassic granitic rocks in the Istanbul and Sakarya zones. Triassic detrital zircons are also common in the Lower Cretaceous, Jurassic and Triassic sandstones of the Sakarya Zone (Okay et al. 2013; Ustaömer et al. 2016; Akdoğan et al. 2018, 2019). This apparent paradox is solved by invoking a subsurface Triassic arc north of the Black Sea, for which there is also some subsurface evidence (Okay and Nikishin 2015). The Triassic arc was adjacent to the Pontides before the Late Cretaceous opening of the Black Sea as a back-arc basin (Görür 1988; Okay et al 1994). This implies that the Triassic detrital zircons in the Upper Cretaceous sandstones were recycled from the Mesozoic sandstones.

Detrital zircon data from the Upper Cretaceous sandstones of the Anatolide–Tauride Block

Samples for detrital zircon study were collected from the Bornova Flysch Zone, which is the main non-metamorphic unit in the northwestern part of the Anatolide–Tauride Block (Fig. 5). The geology of the Bornova Flysch Zone is briefly described below.

Bornova flysch zone

The Bornova Flysch Zone is located between the İzmir–Ankara–Erzincan suture and the metamorphic zones of the Anatolide–Tauride Block (Fig. 1). It consists mainly of deformed olistostromes with Mesozoic limestone and ophiolitic blocks in a greywacke matrix of latest Cretaceous to Paleocene age (Okay and Siyako 1993; Aldanmaz et al. 2008; Okay et al. 2012; Solak et al. 2015). North of Kuşadası the olistostromes lie with a low angle tectonic contact over the Cycladic metamorphic complex and over the Menderes Massif (Fig. 5, Başarır and Konuk 1981).

The age of the carbonate blocks in the Bornova Flysch Zone ranges from Triassic to Late Cretaceous, and there are both shallow marine and deep marine limestone blocks. The ophiolitic blocks include serpentinite, gabbro, basalt and associated radiolarian chert and pelagic shale. Radiolaria from the cherts indicate Triassic, Jurassic and Cretaceous ages (Tekin and Göncüoğlu 2007; Tekin et al. 2012).

The matrix of the blocks consists of strongly sheared greywacke and shale, called as the Bornova Flysch. The clastic rocks make up one third to half of the outcrops in the Bornova Flysch Zone. The greywackes are greenish gray, black in fresh outcrops, and when bedding is recognized, they are medium to thickly bedded, and commonly laminated; the greywackes are intercalated with greenish-gray laminated shales. Four sandstone samples from the matrix of the olistostromes were collected for detrital zircon study (Fig. 5).

The youngest blocks in the Bornova Flysch Zone are Campanian in the northeast and Maastrichtian in the southwest, which provide a maximum depositional age for the olistostromes (Okay and Siyako 1993; Okay et al. 2012). In the İzmir–Manisa region, the matrix of the Bornova Flysch Zone includes calcareous shales with thin pelagic limestone intercalations. These have yielded pelagic foraminifera of Middle–Late Maastrichtian and Late Paleocene ages from different localities (Özer and İrtem 1982; Erdoğan 1990a;

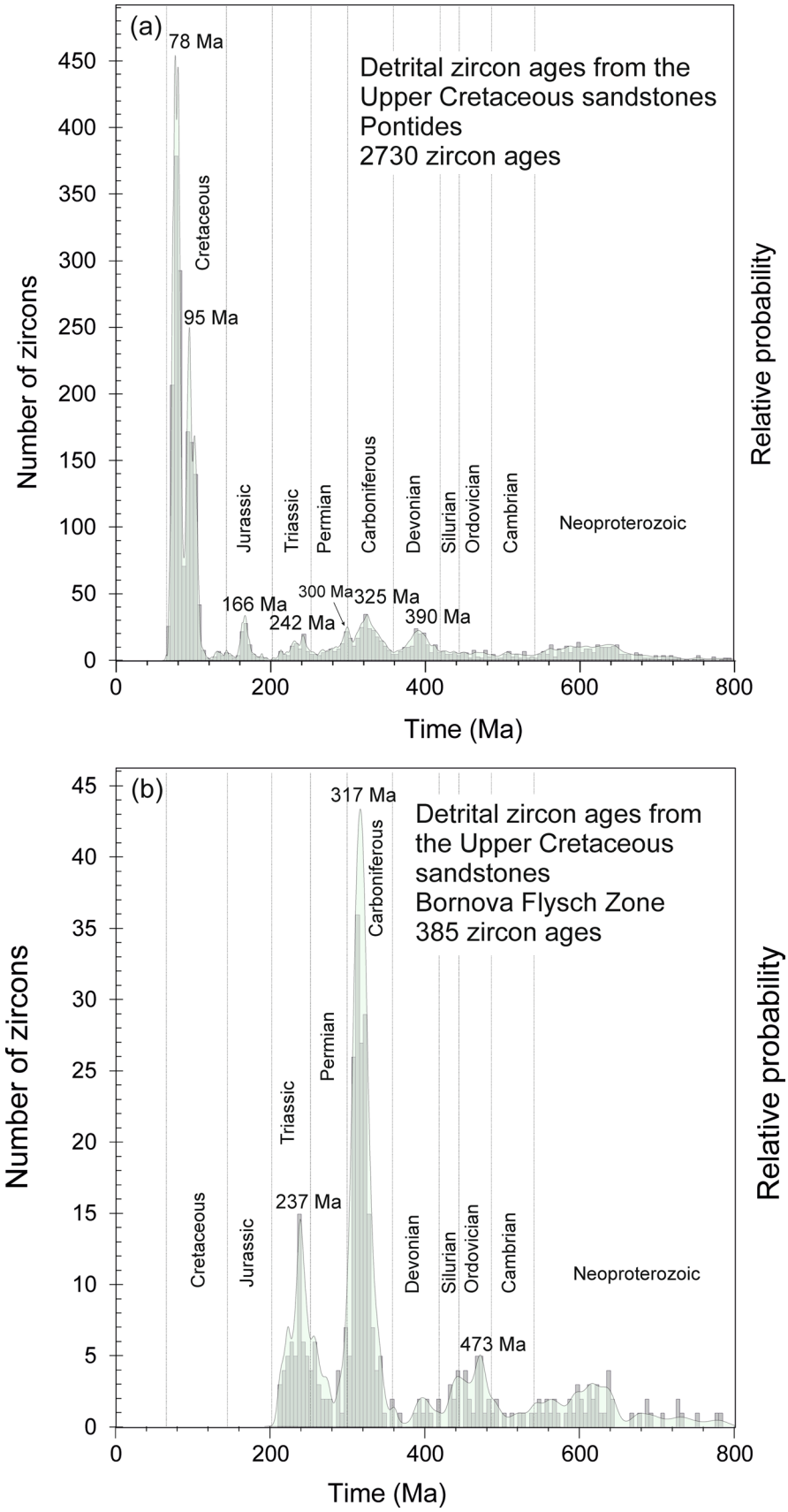

Fig. 6 Detrital zircon ages from the Upper Cretaceous sandstones from the Pontides **a** and the Bornova Flysch of the Anatolide–Tauride Block. **b** The Pontide ages comprise new data as well as ages reported by Akdoğan et al. (2019), Okay et al. (2019, 2020) and Mueller et al. (2022), whereas detrital zircon ages from the Bornova Flysch Zone are from this study only. The bin widths are 2.5 my. For the new analytical data see Table S2

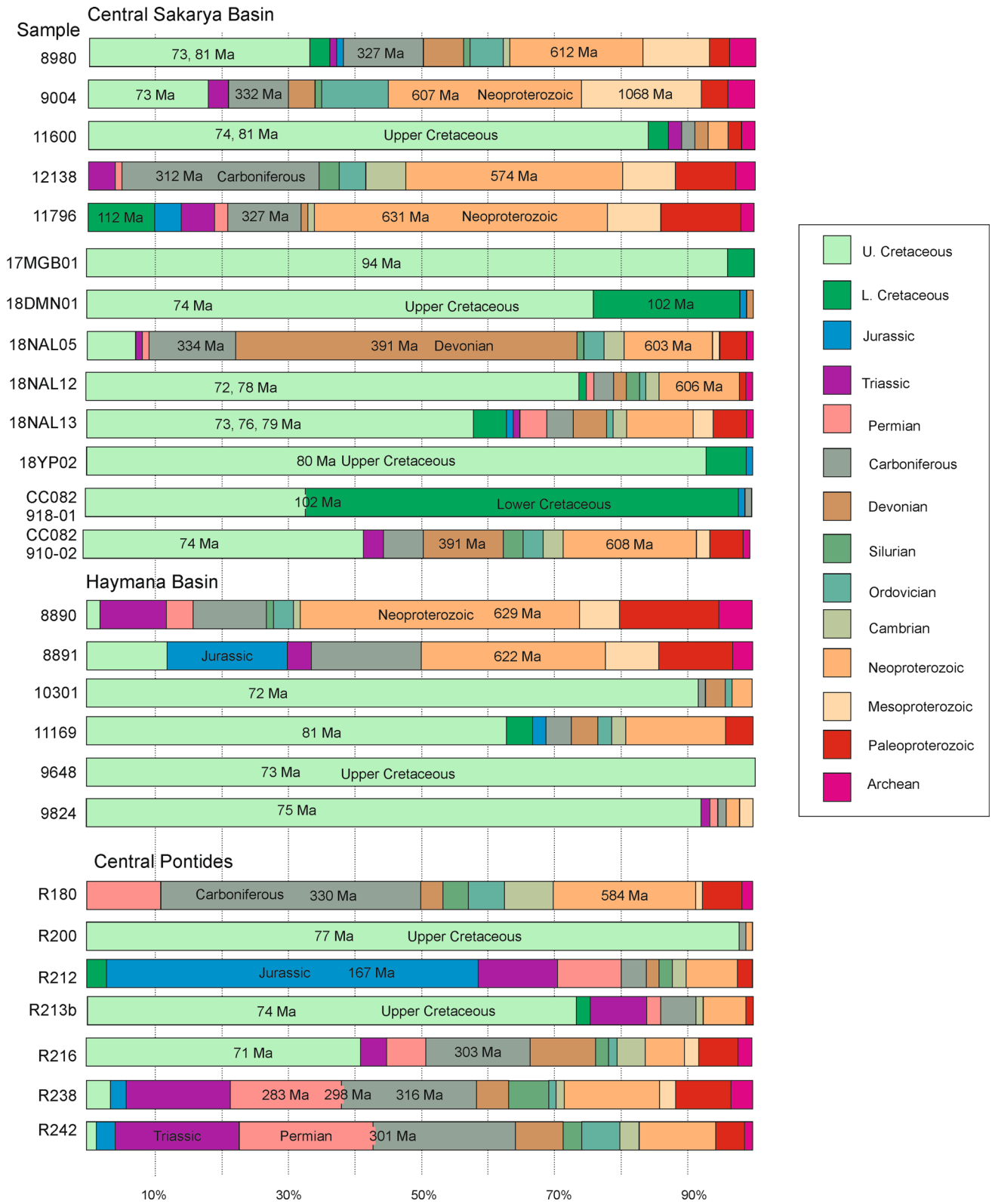

Fig. 7 Percentages of detrital zircon ages from the Upper Cretaceous sandstone samples from the Pontides. The numbers on the charts refer to peak ages

Işıntek et al. 2007; Sarı 2013). Overall, paleontological data indicate a Maastrichtian to Paleocene age for the Bornova Flysch with a possible depositional younging towards the southwest (Okay et al. 2012). An upper limit to its age, as well as to the semi-brittle deformation in the Bornova Flysch Zone is given by the undeformed Lower Eocene (Cuisian, ca. 50 Ma) shallow marine limestones, which lie unconformably over the matrix and blocks of the Bornova Flysch Zone northeast of Akhisar (Fig. 5, Akdeniz 1980).

Karaburun Sequence: Within the Bornova Flysch Zone, a relatively intact Late Paleozoic–Mesozoic sequence crops out on the Karaburun peninsula and the adjacent island of Chios (Fig. 5). Stratigraphically the lowest part Karaburun–Chios series consist of strongly deformed Upper Carboniferous–Lower Permian greywacke and shale with Silurian, Devonian and Carboniferous limestone and chert blocks (Kozur 1998; Groves et al. 2003; Zanchi et al. 2003; Çakmakoğlu and Bilgin 2006; Robertson and Ustaömer 2009; Löwen et al. 2017). This Karaburun Melange is interpreted as a Late Paleozoic subduction–accretion complex (Robertson and Picket 2000). It is intruded by small Triassic granitic bodies (ca. 245 Ma, Akal et al. 2011, Ustaömer et al. 2016), and is overlain by an over 4 km thick Triassic to Lower Cretaceous sedimentary sequence dominated by shallow marine carbonates (Besenecker et al. 1968; Jacobshagen 1972; Brinkmann et al. 1972; Erdoğan et al. 1990; Masse and Işıntek 2000). Many of the blocks in the Bornova Flysch Zone can be correlated with these Mesozoic shallow marine limestones.

The Mesozoic carbonates of the Karaburun sequence are unconformably overlain by Upper Cretaceous (Campanian–Maastrichtian) pelagic limestones and siliciclastic turbidites. The uplift and erosion prior to the deposition of the pelagic limestones is related to the tectonic emplacement of ophiolite and continental margin units over the Anatolide–Tauride carbonate platform during the Campanian (Okay and Siyako 1993; Robertson et al. 2009). In many composite blocks in the Bornova Flysch Zone, Upper Cretaceous pelagic limestones also lie unconformably over Triassic or Jurassic carbonates (Okay and Altıner 2007; Okay et al. 2012).

The Upper Cretaceous series in the Karaburun peninsula is best known from the Balıklıova region in the eastern part of the peninsula (Figs. 5 and 8). Here, the sequence starts with basal conglomerates, which lie unconformably over the Triassic shallow marine limestones (Fig. 8). The conglomerates are overlain by red pelagic limestones of early Campanian to early Maastrichtian age (84–70 Ma), which pass up into a turbidite sequence of shale, sandstone and siltstone (Brinkmann et al. 1977; Erdoğan 1990b; Çakmakoğlu and Bilgin 2006). The turbidite series includes clasts of Mesozoic limestone. It has a minimum thickness of 500 m and is tectonically overlain by Triassic carbonates (Fig. 8). Balıklıova area is one of the few localities, where the stratigraphic relation between the siliciclastic turbidites and the underlying Mesozoic carbonate sequence is exposed (Erdoğan 1990b). A similar transition from carbonates to Lower Paleocene siliciclastic turbidites is also described from some of the larger carbonate blocks in the Bornova and Manisa region (Konuk 1977; Özer and İrtem 1982; Poisson and Şahinci 1988; Solak et al. 2015). Compared to the matrix of the Bornova Flysch Zone, such turbidites are less deformed and form part of a coherent sequence; they probably correspond to an early stage of the deposition of the olistostromes. A sandstone sample (13,440) was collected from the Balıklıova turbidites for detrital zircon study (Fig. 8).

Detrital zircon ages from the Bornova Flysch Zone

We obtained 692 dates from detrital zircons from five Upper Cretaceous sandstone samples from the Bornova Flysch of which 378 were concordant within 10% (55%; Table S3). The samples come from a large area of 180 km by 50 km (Fig. 5); four samples are collected from the matrix of the Bornova Flysch Zone and one sample (13,440) from the Maastrichtian sandstones from the Balıklıova area (Fig. 8). Most of the detrital zircons are euhedral to subhedral and show zoning in CL images (Fig. S2) indicating a magmatic origin. The biostratigraphically determined depositional ages of the sandstone samples are Maastrichtian in the southwest (samples 555 and 13,440) and Campanian–Maastrichtian in the northeast (samples 10,349, 10,350, 10,353).

Figure 6b shows the detrital zircon ages from the Bornova Flysch. A striking feature is the absence of Cretaceous and Jurassic zircons. This is in major contrast to the Pontide Upper Cretaceous sandstones, where the dominant zircon population is of Late Cretaceous age and the Jurassic zircons form a major population (Fig. 6a). The major Phanerozoic zircon ages in the Bornova Flysch are Carboniferous (159 zircons, 41.3%), Triassic (50 zircons, 13.0%), Permian (28 zircons 7.3%) and Ordovician (22 zircons, 5.7%) (Fig. 6b). Late Carboniferous and Middle Triassic zircons form conspicuous age peaks at 317 Ma and 237 Ma, respectively (Fig. 6b). Neoproterozoic zircons (63 zircons, 16.4%) form a broad age plateau between 540 and 650 Ma, similar to that observed in the Pontide equivalents. Mesoproterozoic to Archean zircons (37 grains) constitute 9.6% of the whole zircon population.

Figure 9 shows the detrital zircon ages from individual samples from the Bornova Flysch Zone. There is little variation among the samples in terms of detrital zircon ages. Carboniferous zircons form the dominant population in all five samples, the peak ages are Late Carboniferous (320–309 Ma). The Triassic zircons are also significant in all samples with Middle Triassic peak ages of 239–238 Ma

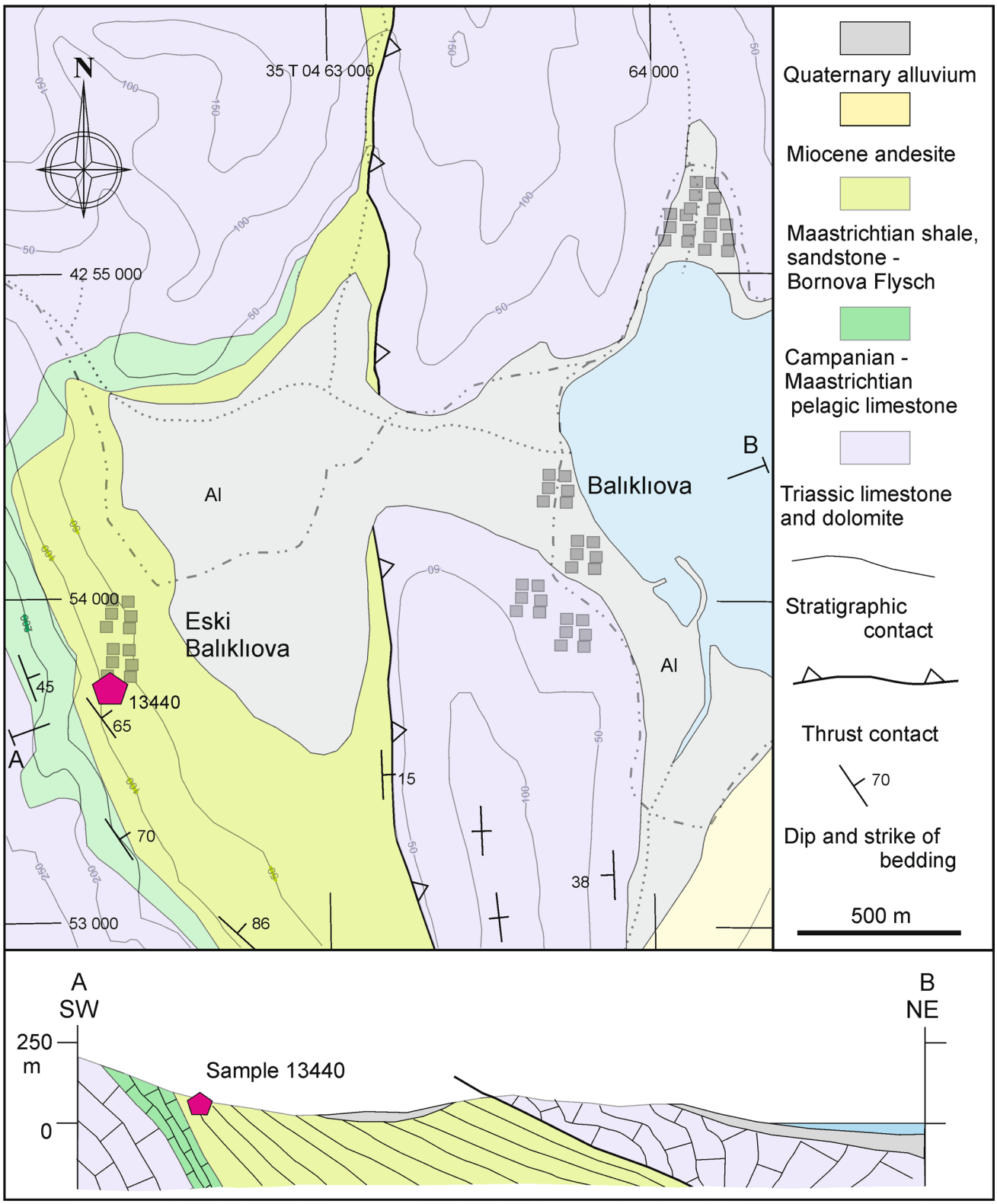

Fig. 8 Geological map and cross-section of the Balıklıova region on the Karaburun peninsula, where the stratigraphic base of the Bornova Flysch crops out (modified from Brinkmann et al. 1977 and Erdoğan 1990b). For location see Fig. 5

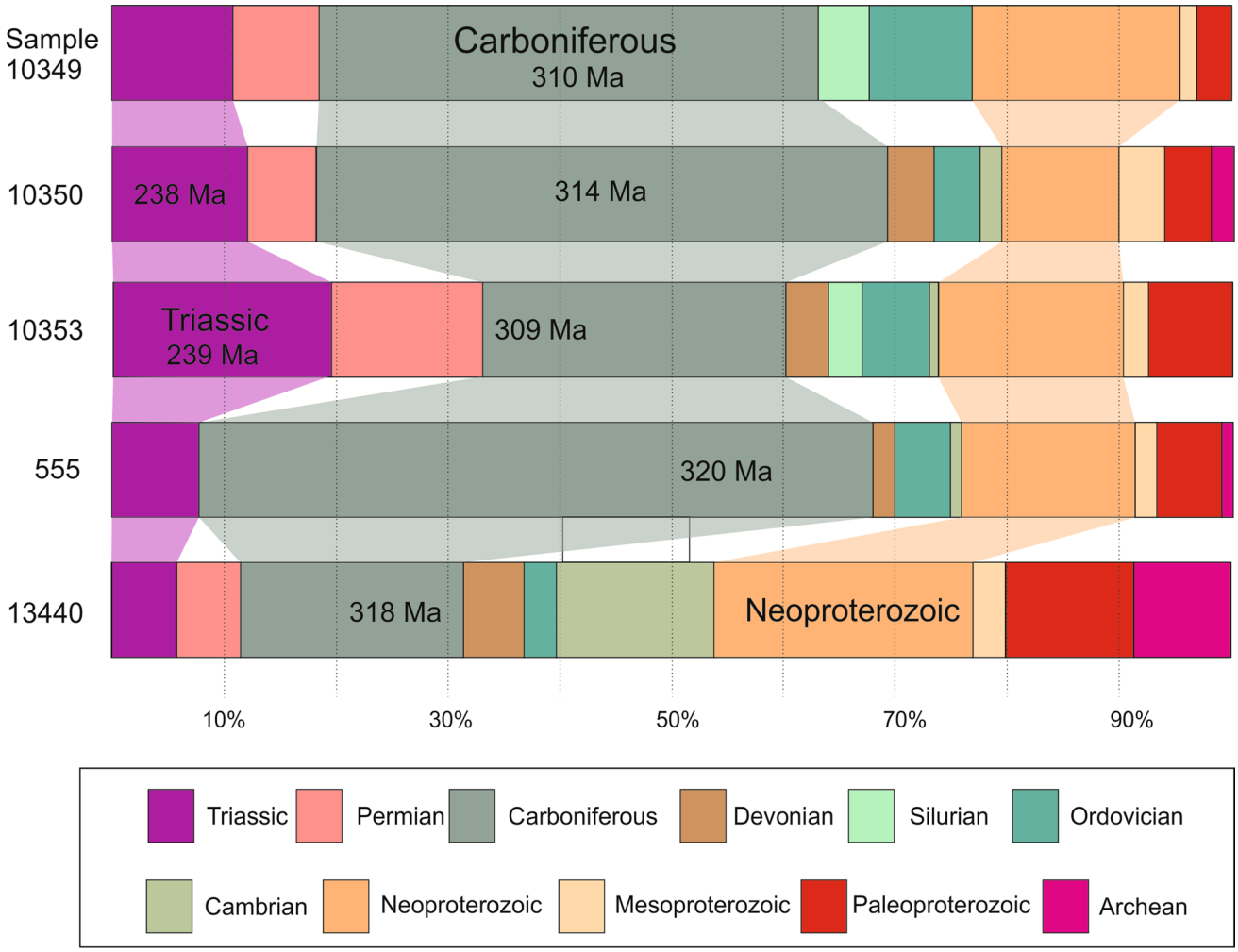

Fig. 9 Percentages of detrital zircon ages from the Upper Cretaceous sandstone samples from the Bornova Flysch Zone. The numbers on the charts refer to peak ages. The samples are arranged from north to south

(Fig. 9). The Balıklıova sandstone sample (13,440) shows a similar detrital age spectra as the sandstone samples taken from the matrix of the olistostromes, which suggest that the Bornova Flysch was deposited on top of the Mesozoic carbonate platform prior to intense semi-brittle deformation.

Detrital zircons in the Bornova Flysch were derived both from magmatic and clastic sedimentary rocks. The most likely clastic sedimentary source is the Upper Carboniferous – Lower Permian Karaburun Melange. The detrital zircon record of the Karaburun Melange was studied in detail by Löwen et al. (2017) and Ustaömer et al. (2020). The dominant detrital zircon population in the Karaburun Melange is Cambrian–Neoproterozoic (45–50%) followed by Devonian (5–15%), Carboniferous (1–15%) and Ordovician (2–5%). It is likely that most of the Cambrian–Neoproterozoic, Devonian and Ordovician detrital zircons in the Bornova Flysch were recycled from the matrix turbidites of the Karaburun Melange. On the other hand, the Carboniferous detrital zircons are much more abundant in the Bornova Flysch (41% of the total detrital zircon population) than in the Karaburun Melange (1–15% of the total detrital zircon population), which suggests that the majority of the Carboniferous detrital zircons in the Bornova Flysch were derived from Carboniferous magmatic rocks.

Petrography and detrital modes of the Upper Cretaceous sandstones

Twelve samples of Upper Cretaceous sandstones from the Pontides and the Bornova Flysch were petrographically studied and point counted. These include 11 samples analyzed for detrital zircons. The location of the samples is shown in Fig. 2 and their coordinates are given in Table S2. The point-counted sandstones are free of penetrative strain and recrystallization. The point counting was done using

Gazzi-Dickinson method (e.g., Dickinson 1970; Ingersoll et al. 1984) with sand-sized (> 0.03 mm) monomineralic components of lithic fragments counted as individual mineral grains, and only aphanitic grains (< 0.03 mm) are classified as lithic clasts. More than 400 framework grains were counted in each section. Petrographic counting parameters and modal point-count data are presented in Table S4.

Petrographically, the Upper Cretaceous sandstones from the Pontides are lithic arenites with poorly sorted, angular to subangular lithic (average 41 modal %), quartz (20%), calcite (21%) and feldspar (15%) grains and minor matrix (3%) (Fig. 10). Minor constituents (< 0.5%) include opaque, muscovite, epidote and glaucophane. The lithic grains are predominantly volcanic (90%) with minor phyllite (10%). Calcite is common in all samples and occurs both as micritic and sparitic grains. Some of the sparry calcite also acts as cement. Petrographically the sandstones are similar to those described from the Central Pontides by Akdoğan et al. (2019) and all but one sample plot in the magmatic arc field in the QFL tectonic discrimination of Dickinson et al. (1983). The one sample (8890), which plots in the recycled orogen field, comes from the stratigraphic base of the Haymana Formation and contains predominantly pre-Cretaceous zircons (Fig. 7). The detrital zircon ages and petrography indicate that the Pontide sandstones were mainly sourced from the magmatic arc; however, presence of minor glaucophane and low-grade metamorphic rocks shows that the accretionary complex was also providing detritus to the forearc basin.

Sandstones from the Bornova Flysch are lithic arenites and feldspathic litharenites (Fig. 10). They consist of poorly sorted angular to subangular quartz (average 39 modal %), lithic (24%), feldspar (21%), and calcite (5%) grains surrounded by fine-grained matrix (11%). Minor constituents (< 0.5%) include opaque, muscovite, chlorite, and biotite. Sandstones from the Bornova Flysch have a higher amount of matrix (average 11%), more quartz and lesser lithic grains compared to those from the Pontides (Fig. 10). Micritic and sparitic calcite occurs only in some samples, and is significant only in the Balıklıova sample (13,440). Lithic grains are mainly volcanic (74%) and phyllite (23%). In the discrimination diagram, sandstones from the Bornova Flysch Zone plot in the field of recycled orogen (Fig. 10).

Discussion

Late Cretaceous paleogeography and tectonics

A Late Cretaceous magmatic arc can be followed along the southern margin of the Black Sea (Fig. 2). It formed as a result of northward subduction of the İzmir–Ankara–Erzincan ocean under the Pontides. The magmatic arc was bordered in the south by forearc basins with thick sequences of volcaniclastic sandstone and shale (Görür et al. 1998; Ocakoğlu et al. 2019; Kandemir et al. 2019; Mueller et al. 2022). Bedrock magmatic and detrital zircon ages indicate that arc magmatism peaked in the Campanian (ca. 78 Ma) and was reduced drastically in the Maastrichtian (ca. 70 Ma, Figs. 4a, 6a). The arc volcanic rocks are commonly overlain by Maastrichtian to Lower Eocene limestone and marl, and the forearc basins show a regressive development with the turbidites passing up into shallow marine sandstones and into Paleocene red beds (e.g., Ocakoğlu et al. 2019).

In contrast to the Pontides, the Anatolide–Tauride Block formed an isolated carbonate platform during the Mesozoic surrounded by the northern and southern branches of the Tethys ocean (Fig. 11). During the Late Cretaceous (ca. 95 Ma) an intra-oceanic subduction zone was initiated in the İzmir–Ankara–Erzincan ocean north of the Anatolide–Tauride Block, as suggested by the ages of the subophiolite metamorphic rocks (Fig. 12a, e.g., Parlak et al. 2013; Xin et al. 2022). Later in the Late Cretaceous (Campanian, ca. 80 Ma), the northern margin of the Anatolide–Tauride Block was subducted in this intra-oceanic subduction zone and underwent HP/LT regional metamorphism (Fig. 12b; Okay and Whitney 2010; Plunder et al. 2015). In the more southerly parts of the Anatolide–Tauride Block, the continental subduction manifested itself as a major ophiolite obduction. The obducted ophiolite had a north–south length of more than 400 km, and covered most of the Anatolide–Tauride Block (e.g., Dilek et al. 1999). It was bounded in the west by a tear fault, the Bornova Fault (Fig. 12). The presence of such a fault is indicated by the following observations (Okay et al. 2012): a) the Late Cretaceous ophiolite obduction does not extend into Greece and the Aegean islands, b) the western margin of the Bornova Flysch Zone is largely free of ophiolite blocks (Fig. 5), c) The İzmir–Ankara–Erzincan suture, which has an overall east–west trend, forms a sharp NNE trending bend between İzmir and Balıkesir (Fig. 1). An oblique foreland basin was created west of the Bornova Fault, where the olistostromes of the Bornova Flysch Zone were deposited (Fig. 12, Okay et al. 2012).

The presence of Neoproterozoic, Paleozoic and Triassic detrital zircons in the Bornova Flysch (Fig. 9) indicates that basement rocks were on the surface during the Late Cretaceous. The uplift of the basement of the Anatolide–Tauride Block can be related to the thrusting associated with the ophiolite obduction (Fig. 12c).

In the early paleomaps of the Tethyan region (e.g., Robertson and Dixon 1984; Dercourt et al. 1986), the İzmir–Ankara–Erzincan ocean is shown to separate the Pontides and the Anatolide–Tauride Block in the Late Cretaceous (75–70 Ma), whereas more recently published paleomaps (e.g., Moix et al. 2008; Robertson et al. 2013; Barrier et al. 2018) show collision between these two continental

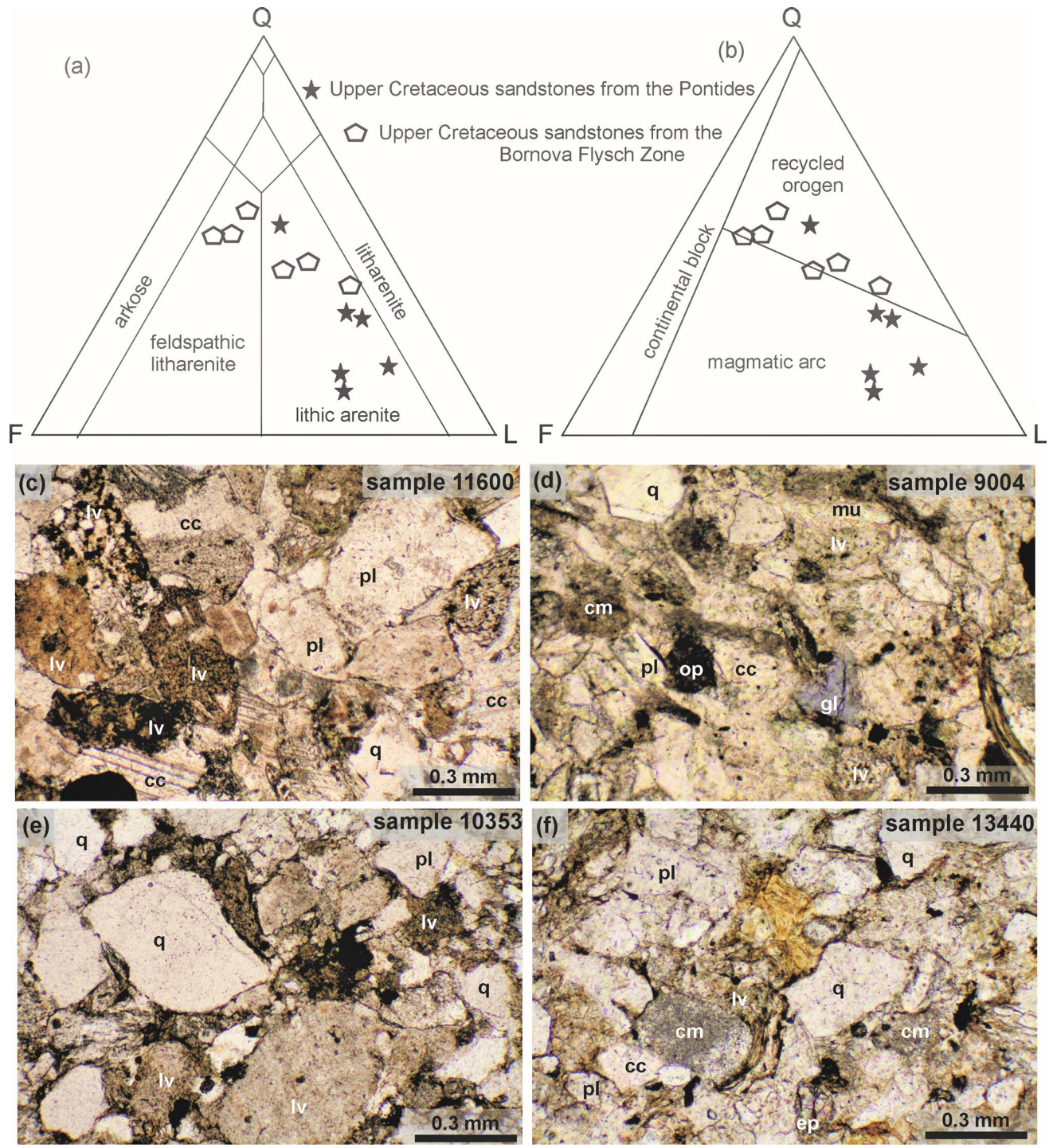

Fig. 10 Modal compositions and microphotos of the sandstones from the Pontides and the Bornova Flysch Zone. **a** Quartz (Q) – feldspar (F) – lithic (L) diagram. **b** QFL tectonic discrimination diagram after Dickinson et al. (1983). Representative plane-polarized light microphotos of the Upper Cretaceous sandstones from the Pontides (**c** and **d**) and from the Bornova Flysch Zone (**e** and **f**). Abbreviations: cc sparry calcite, cm micritic calcite, ep epidote, gl glaucophane, lv volcanic lithic, mu muscovite, pl plagioclase, q quartz

terranes starting already in Late Cretaceous (75–70 Ma). The absence of Jurassic and Cretaceous zircons in the Bornova Flysch implies the existence of a wide Tethyan ocean separating the Pontides and the Anatolide–Tauride Block during the Late Cretaceous giving support to early paleomaps (Fig. 12).

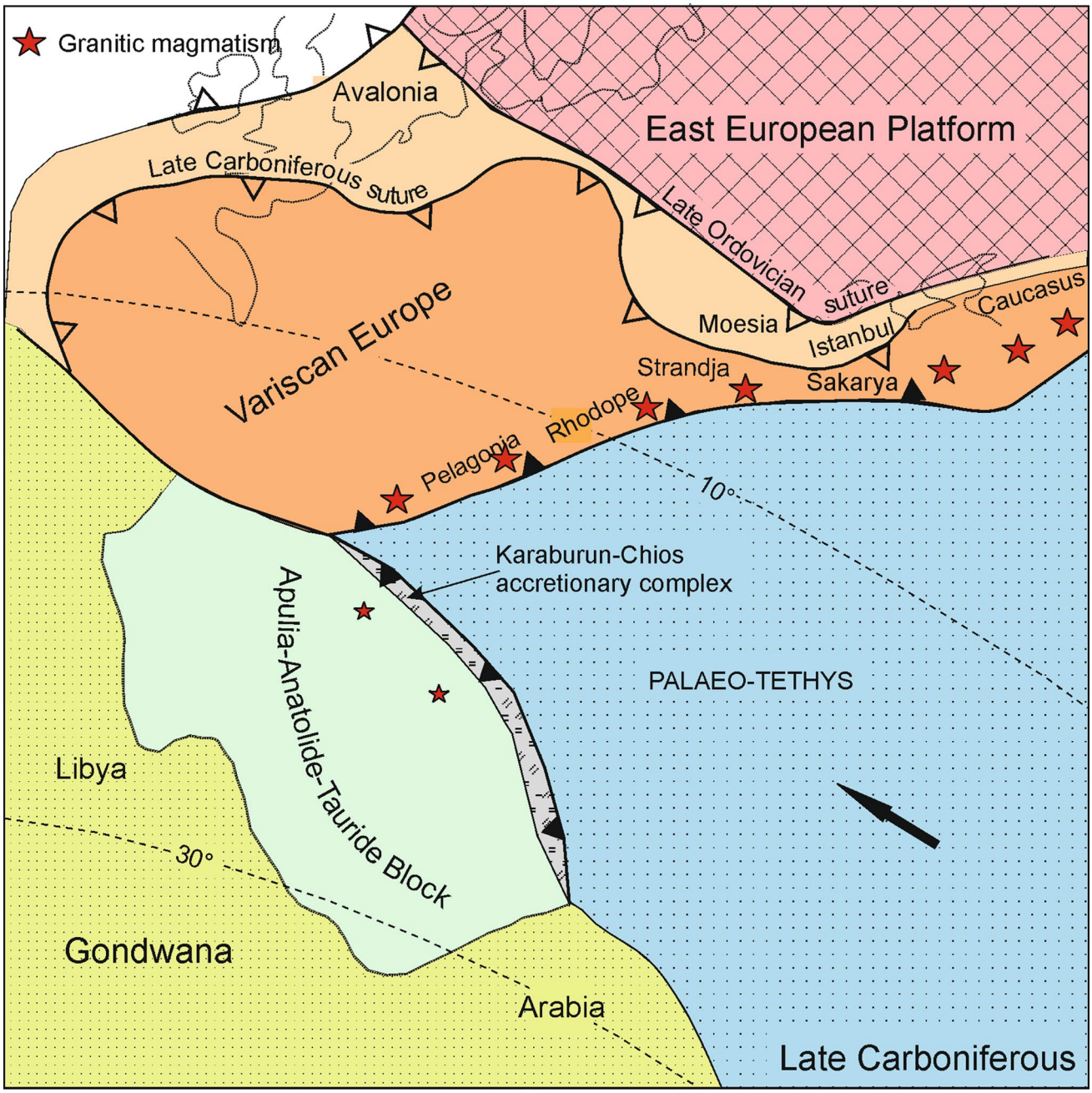

Fig. 11 Paleogeographic map for the Late Carboniferous showing possible locations of the Pontides (Sakarya and Istanbul zones), the Anatolide–Tauride Block and the Chios–Karaburun Upper Paleozoic subduction–accretion complex (modified from Okay et al. 2006 and Robertson and Ustaömer 2009)

Magmatic record of the Anatolide–Tauride Block

The absence of Cretaceous and Jurassic detrital zircons in the Bornova Flysch implies that the detrital zircons in the Bornova Flysch must have been derived from the Anatolide–Tauride Block, and therefore, they provide a proxy for magmatism in the Anatolide–Tauride Block. Detrital zircon record from the Bornova Flysch indicates Late Carboniferous (ca. 317 Ma), Middle Triassic (ca. 237 Ma), Devonian (473 Ma), and late Neoproterozoic magmatic events. Neoproterozoic metagranites are exposed over large areas in western Anatolia (Fig. 5); however, they make up a minor component of the detrital zircon record, and were probably recycled from the Karaburun Melange. This is in accordance with the Miocene exhumation of the Menderes Massif (e.g., Gessner et al. 2001). Carboniferous and

Triassic detrital zircon ages correlate with the coeval magmatism in the Anatolide–Tauride Block (cf. Figure 4b and 5b). Carboniferous detrital zircons form the major population in the Bornova Flysch, which shows that Carboniferous magmatic rocks must have been more widespread on the surface during the Late Cretaceous then at the present day.

Carboniferous detrital zircons and magmatic rocks are common both in the Pontides and in the Anatolide–Tauride Block (Figs. 4 and 6); thus, they are not diagnostic for Pontide or Anatolide–Tauric provenance. However, the εHf(t) values of the Carboniferous zircons from the Pontides and the Anatolide–Tauride Block appear to be different (cf. Figure 14 of Ustaömer et al. 2020). Devonian detrital zircons indicate a coeval magmatic activity, which is unknown from the Anatolide–Tauride Block.

Significance of Carboniferous detrital zircons

Carboniferous granites are widespread in the Pontides and in the Variscan Europe, on the other hand, there are rare on the northern Gondwana margin. Consequently, Upper Paleozoic sedimentary sequences with significant Carboniferous zircon populations, such as those of Chios and Karaburun, are commonly placed on the southern margin of Laurasia, (e.g., Meinhold et al. 2008; Löwen et al. 2017). However, in both Chios and Karaburun the Upper Paleozoic series are stratigraphically overlain by Mesozoic carbonates, which are a typical stratigraphic feature of the Anatolide–Tauride Block (e.g., Erdoğan et al. 1990; Robertson and Pickett 2000).

The Bornova Flysch was clearly deposited in the Anatolide–Tauride Block during the latest Cretaceous and Paleocene. Yet, the dominant detrital zircon population in the Bornova Flysch is Carboniferous in age, and makes up 41% of the detrital zircons. A recycled origin for all the Carboniferous zircons is highly unlikely since in the Karaburun Melange, the Carboniferous zircons constitute only 1–15% of the zircon population (Löwen et al. 2017; Ustaömer et al. 2020). Therefore, it is very likely that the Bornova Flysch was partly sourced from Carboniferous magmatic rocks, similar to those described from the Afyon Zone of the Anatolide–Tauride Block (Fig. 5, Candan et al. 2016). Carboniferous granites are also described from northwest Iran (e.g., Bea et al. 2011; Moghadam et al. 2015) pointing to Carboniferous magmatism on the northern margin of Gondwana possibly linked to short-lived southward subduction (Fig. 10; Robertson and Ustaömer 2009; Candan et al. 2016). Therefore, the source of Carboniferous detrital zircons in the Bornova Flysch and in other units of the Anatolide–Tauride Block lies in Gondwana, as was also suggested by Ustaömer et al. (2020). An additional argument for the Gondwanian origin of the detrital zircons in the Anatolide–Tauride Block is provided by the εHf(t) data. The εHf(t) values of zircons from the Carboniferous zircons from the Pontides and the Anatolide–Tauride Block are different, and the detrital Carboniferous zircons from the Anatolide–Tauride Block have εHf(t) values similar to those from the Carboniferous Anatolide–Tauride granites (Fig. 14 of Ustaömer et al. 2020).

Conclusions

1. Uppermost Cretaceous (75–70 Ma) turbidites of the Anatolide–Tauride Block do not contain any Jurassic and Cretaceous detrital zircons, which are common in the age-equivalent sandstones of the Pontides. This shows that there was no sediment transport across the Tethyan ocean during this time. More specifically volcanic detritus of the Late Cretaceous Pontide magmatic arc was not reaching the Anatolide–Tauride Block at 75–70 Ma.
2. The Phanerozoic detrital zircon ages in the Upper Cretaceous sandstones of the Pontides are predominantly Cretaceous (56%) followed by Carboniferous (7.9%), Devonian (5.3%), Jurassic (3.1%) and Triassic (2.9%). In contrast, in the equivalent Phanerozoic detrital zircon populations in the Bornova Flysch Zone of the Anatolide–Tauride Block are Carboniferous (41.3%), Triassic (7.1%), Permian (6.9%) and Devonian (5.3%). The absence of Cretaceous and Jurassic zircons furthermore shows that the deformation of the Bornova Flysch Zone is pre-collisional and is associated with ophiolite obduction.
3. Detrital zircons from the Upper Cretaceous sandstones from the Bornova Flysch Zone show a major Late Carboniferous age peak (327 Ma, 41.3% of the zircon ages). This indicates that Carboniferous magmatism on the northern margin of Gondwana is more widespread than hitherto recognized. Carboniferous detrital zircons also form a significant population (7.9% of the zircon ages) in the Upper Cretaceous sandstones in the Pontides, showing that magmatic activity occurred on both the Eurasian and Gondwana margins during the Carboniferous. Thus, it is not correct to identify a Laurasian origin on the basis of Carboniferous detrital zircons. However, the εHf(t) values of Carboniferous zircons from the Pontides and the Anatolide–Tauride Block appear to be different (Ustaömer et al. 2020).
4. Magmatic bedrock and detrital zircon ages from the Pontides and the Anatolide–Tauride Block show similar Triassic, Paleozoic and Neoproterozoic age patterns (Figs. 4 and 6). The main difference between these two units is the absence of Cretaceous and Jurassic magmatism in the Anatolide–Tauride Block.
5. The Karaburun peninsula in the Bornova Flysch Zone comprises a semi-intact Mesozoic carbonate sequence overlain by Maastrichtian turbidites. Detrital zircons

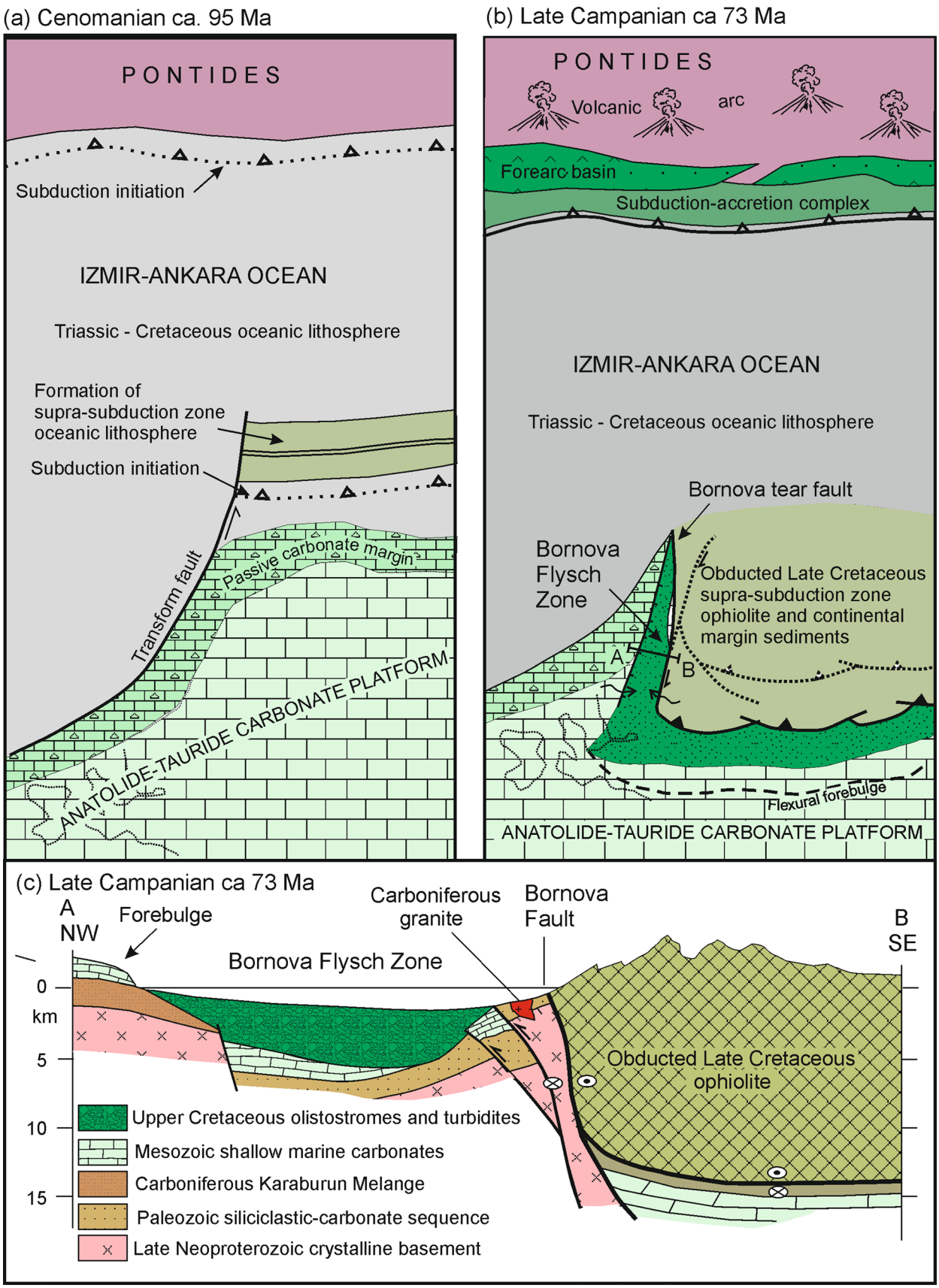
(a) Cenomanian ca. 95 Ma
PONTIDES
Subduction initiation
IZMIR-ANKARA OCEAN
Triassic - Cretaceous oceanic lithosphere
Formation of
supra-subduction zone
oceanic lithosphere
Subduction initiation
Transform fault
Passive carbonate margin
ANATOLIDE-TAURIDE CARBONATE PLATFORM
(b) Late Campanian ca 73 Ma
PONTIDES
Volcanic
arc
Forearc basin
Subduction-accretion complex
IZMIR-ANKARA OCEAN
Triassic - Cretaceous oceanic lithosphere
Bornova tear fault
Bornova
Flysch
Zone
Obducted Late Cretaceous
supra-subduction zone
ophiolite and continental
margin sediments
A
B
Flexural forebulge
ANATOLIDE-TAURIDE CARBONATE PLATFORM
(c) Late Campanian ca 73 Ma
A
NW
Forebulge
Carboniferous
granite
Bornova
Fault
B
SE
Bornova Flysch Zone
0
km
5
10
15
Obducted Late Cretaceous
ophiolite
Upper Cretaceous olistostromes and turbidites
Mesozoic shallow marine carbonates
Carboniferous Karaburun Melange
Paleozoic siliciclastic-carbonate sequence
Late Neoproterozoic crystalline basement

◂**Fig. 12** Late Cretaceous paleogeography. **a** Cenomanian (ca. 95 Ma), initiation of intra-oceanic and Andean-type subduction zones and generation of Late Cretaceous supra-subduction zone oceanic lithosphere. **b** Late Campanian (ca. 73 Ma), obduction of the supra-subduction zone ophiolite over the Anatolide–Tauride Block and the creation of the Bornova Flysch Zone in an oblique foreland basin. In the north arc volcanism and forearc sedimentation in the Pontides. **c** Cross section showing the ophiolite obduction and generation of the Bornova Flysch Zone in an oblique foreland basin (modified from Okay et al. 2012)

from these turbidites show a similar age pattern to those from the matrix of the Bornova Flysch Zone. This suggests that the olistostromes of the Bornova Flysch Zone were originally deposited over the Mesozoic carbonate platform before their deformation in the latest Cretaceous and Paleocene.

Supplementary Information The online version contains supplementary material available at https://doi.org/10.1007/s00531-022-02275-1.

Acknowledgements Aral Okay thanks TÜBİTAK projects 113R007 and 116YR007 and TÜBA for financial support. We thank İsmail İşintek for help in the field in the Karaburun peninsula. Alastair Robertson and Timur Ustaömer provided constructive detailed reviews, which improved the text. We thank Ezgi Saglam, Turgut Duzman and Cemre Ay for help with the compilation of Table S1.

References

Akal C, Koralay OE, Candan O, Oberhänsli R, Chen F (2011) Geodynamic implications of Early Triassic Karaburun Granitoid (Western Turkey) for the opening history of Neo-Tethys. Turk J Earth Sc 20:255–271

Akal C, Candan O, Koralay E, Oberhänsli R, Chen F, Prelevic D (2012) Early Triassic potassic volcanism in the Afyon Zone of the Anatolides/Turkey: implications for the rifting of the Neo-Tethys. Int J Earth Sci 101:177–194

Akdeniz N (1980) Başlamış formation (in Turkish). Jeoloji Mühendisliği 10:39–47

Akdoğan R, Okay AI, Sunal G, Tari G, Meinhold G, Kylander-Clark ARC (2017) Provenance of a large Lower Cretaceous turbidite submarine fan on the active Laurasian margin. J Asian Earth Sc 134:309–329

Akdoğan R, Okay AI, Dunkl I (2018) Triassic-Jurassic arc magmatism in the Pontides as revealed by the U-Pb detrital zircon ages in the Jurassic sandstones northeastern Turkey. Turk J Earth Sc 27:89–109

Akdoğan R, Okay AI, Dunkl I (2019) Striking variation in the provenance of the Lower and Upper Cretaceous turbidites in the central Pontides (northern Turkey) related to the opening of the Black Sea. Tectonics 38:1050–1069

Akgündüz S, Aysal N, Peytcheva I, Yilmaz Şahin S, Güngör Y (2021) Geochronology, geochemistry and tectono-magmatic evolution of the upper Carboniferous–lower Permian Kula pluton in the Istranca (Strandja) Massif, NW Turkey. Geol Carp 72:373–394

Aldanmaz E, Yalınız MK, Güctekin A, Göncüoğlu MC (2008) Geochemical characteristics of mafic lavas from the Neotethyan ophiolites in western Turkey: implications for heterogeneous source contribution during variable stages of ocean crust generation. Geol Mag 145:37–54

Aysal N, Ustaömer T, Öngen S, Keskin M, Köksal S, Peytcheva I, Fanning M (2012) Origin of the Early-Middle Devonian magmatism in the Sakarya Zone, NW Turkey: Geochronology, geochemistry and isotope systematics. J Asian Earth Sc 45:201–222

Aysal N, YılmazŞahin S, Güngör Y, Peytcheva I, Öngen S (2018) Middle Permian–early Triassic magmatism in the Western Pontides, NW Turkey: Geodynamic significance for the evolution of the Paleo-Tethys. J Asian Earth Sc 164:83–103

Barrier E, Vrielynck B, Brouillet J, Brunet M (2018) Paleotectonic Reconstruction of the Central Tethyan Realm. Tectonono-Sedimentary-Palinspastic maps from Late Permian to Pliocene. CCGM/CGMW, Paris

Başarır E, Konuk YT (1981) The crystalline basement and allochthonous units in the Gümüldür region (in Turkish). Türkiye Jeoloji Kurumu Bülteni 24:95–100

Bea F, Mazhari A, Montero P, Amini S, Ghalamghash J (2011) Zircon dating, Sr and Nd isotopes and element geochemistry of the Khalifan pluton, NW Iran: evidence for Variscan magmatism in a supposedly Cimmerian superterrane. J Asian Earth Sci 40:172–179

Besenecker H, Dürr S, Herget G, Jacobshagen V, Kauffmann G, Lüdtke G, Roth W, Tietze KW (1968) Geologie von Chios (Agais). Geol Palaeontol 2:121–150

Bonev N, Filipov P, Raicheva R, Moritz R (2022) Evidence of late palaeozoic and middle triassic magmatism in the Sakar-Strandzha Zone SE Bulgaria: regional geodynamic implications. Int Geol Rev 64:1199–1225

Brinkmann R, Flügel E, Jacobshagen V (1972) Trias Jura und Unterkreide der Halbinsel Karaburun (West-Anatolien). Geol Palaeontol 6:139–150

Brinkmann R, Gümüş H, Plumhoff F, Salah AA (1977) Höhere Oberkreide in Nordwest-Anatolien und Thrakien. N Jb Geol Paleont Abh 154:1–20

Bröcker M, Enders M (2001) Unusual bulk-rock compositions in eclogite-facies rocks from Syros and Tinos (Cyclades Greece): implications for U-Pb zircon geochronology. Chem Geol 175:581–603

Çakmakoğlu A, Bilgin ZR (2006) Pre-Neogene stratigraphy of the Karaburun peninsula (W of İzmir Turkey). Bull Mineral Res Explor 132:33–61

Candan O, Koralay OE, Akal C, Kaya O, Oberhansli R, Dora OO, Konak N, Chen F (2011) Supra-Pan-African unconformity between core and cover series of the Menderes Massif/Turkey and its geological implications. Precamb Res 184:1–23

Candan O, Akal C, Koralay OE, Okay AI, Oberhänsli R, Prelević D, Mertz-Kraus R (2016) Carboniferous granites on the northern margin of Gondwana Anatolide-Tauride Block Turkey - evidence for southward subduction of Paleotethys. Tectonophysics 683:349–366

Çetinkaplan M, Candan O, Oberhänsli R, Sudo M, Cenki-Tok B (2020) P-T–t evolution of the Cycladic Blueschist Unit in Western Anatolia/Turkey: Geodynamic implications for the Aegean region. J Metamorph Geol 38:379–419

Chen F, Siebel W, Satır M, Terzioğlu N, Saka K (2002) Geochronology of the Karadere basement (NW Turkey) and implications for the geological evolution of the Istanbul Zone. Int J Earth Sc 91:469–481

Çimen O, Göncüoğlu MC, Simonetti A, Sayit K (2017) Whole rock geochemistry, Zircon U-Pb and Hf isotope systematics of the Çangaldağ Pluton: evidences for Middle Jurassic Continental Arc Magmatism in the Central Pontides, Turkey. Lithos 290–291:136–158

Dean WT, Monod O, Rickards RB, Demir O, Bultynck P (2000) Lower Palaeozoic stratigraphy and palaeontology, Karadere-Zirze area, Pontus Mountains, northern Turkey. Geol Mag 137:555–582

Dercourt J, Zonenshain LP, Ricou LE, Kazmin VG, Le Pichon X, Knipper AL, Grandjacquet C, Sbortshikov IM, Geyssant J, Lepvrier C (1986) Geological evolution of the Tethys belt from the Atlantic to the Pamirs since the Lias. Tectonophysics 123:241–315

Dickinson WR (1970) Interpreting detrital modes of greywacke and arkose. J Sed Petrol 40:695–707

Dickinson WR, Beard LS, Brakenridge GR, Erjavec JL, Ferguson RC, Inman KF, Knepp RA, Lindberg FA, Ryberg PT (1983) Provenance of North American Phanerozoic sandstones in relation to tectonic setting. Geol Soc Am Bull 94:222–235

Dilek Y, Thy P, Hacker B, Grundvig S (1999) Structure and petrology of Tauride ophiolites and mafic dyke intrusions (Turkey): implications for the Neotethyan ocean. Geol Soc Am Bull 111:1192–1216

Dokuz A, Gücer MA, Karslı O, Yi K (2022) From Cadomian back-arc basin to Rheic Ocean closure: the geochronological records of the Kurtoğlu Massif, eastern Sakarya Zone, Turkey. Int J Earth Sc 111:1333–1355

Erdoğan B (1990a) Stratigraphic features and tectonic evolution of the İzmir-Ankara Zone in the region between İzmir and Seferihisar (in Turkish). Türkiye Petrol Jeologları Derneği Bülteni 2:1–20

Erdoğan B (1990b) Tectonic relations between İzmir-Ankara Zone and Karaburun belt. Bull Mineral Res Explor 110:1–15

Erdoğan B, Altıner D, Güngör T, Özer S (1990) The stratigraphy of the Karaburun peninsula. Bull Mineral Res Explor 111:1–23

Erkül ST, Sözbilir H, Erkül F, Helvacı C, Ersoy Y, Sümer Ö (2008) Geochemistry of I-type granitoids in the Karaburun Peninsula, West Turkey: evidence for Triassic continental arc magmatism following closure of the Palaeotethys. Island Arc 17:394–418

Eyuboglu Y, Dudas FO, Santosh M, Xiao Y, Yi K, Chatterjee N, Wu F-Y, Bektaş O (2016) Where are the remnants of a Jurassic ocean in the eastern Mediterranean region? Gond Res 33:63–91

Gehrels G (2014) Detrital zircon U-Pb geochronology applied to tectonics. Ann Rev Earth Planet Sci 42:127–149

Gessner K, Ring U, Johnson C, Hetzel R, Passchier CW, Güngör T (2001) An active bivergent rolling-hinge detachment system: Central Menderes metamorphic core complex in western Turkey. Geology 29:611–614

Gessner K, Collins AS, Ring U, Güngör T (2004) Structural and thermal history of poly-orogenic basement: U-Pb geochronology of granitoid rocks in the southern Menderes Massif, Western Turkey. J Geol Soc London 161:93–101

Görür N (1988) Timing of opening of the Black Sea basin. Tectonophysics 147:247–262

Görür N, Tüysüz O, Şengör AMC (1998) tectonic evolution of the central anatolian basins. Int Geol Rev 40:831–850

Groves JR, Larghi C, Nicora A, Rettori R (2003) Mississippian (Lower Carboniferous) microfossils from the Chios Mélange (Chios Island Greece). Geobios 36:379–389

Gücer MA, Arslan M, Sherlock S, Heaman LM (2016) Permo-Carboniferous granitoids with Jurassic high temperature metamorphism in Central Pontides, Northern Turkey. Mineral Petrol 110:943–964

Gutnic M, Monod O, Poisson A, Dumont J-F (1979) Géologie des Taurides Occidentales (Turquie). Mémoires de la Société Géologique de France No 137 112 pp

Hetzel R, Reischmann T (1996) Intrusion age of Pan-African augen gneisses in the southern Menderes Massif and the age of cooling after Alpine ductile extensional deformation. Geol Mag 133:565–572

Ingersoll RV, Bullard TF, Ford RL, Grimm JP, Pickle JD, Sares SW (1984) The effect of grain size on detrital modes: a test of the Gazzi-Dickinson point-counting method. J Sed Petrol 54:103–116

Işıntek İ, Altıner D, Altıner SÖ (2007) Foraminiferal and algal biostratigraphy and paleogeographic implications of the Mesozoic carbonate bodies between İzmir and Soma (Manisa). TÜBİTAK report, 213 pp (unpublished). Accessed 26 May 2022

Jacobshagen V (1972) Die Trias der mittleren Ost-Agais und ihre palaogeographischen Beziehungen innerhalb der Helleniden. Z Deutsch Geol Ges 123:445–454

Kandemir Ö, Akbayram K, Çobankaya M, Kanar F, Pehlivan Ş, Tok T, Hakyemez A, Ekmekçi E, Danacı F, Temiz U (2019) From arc evolution to arc-continent collision: Late Cretaceous–middle Eocene geology of the Eastern Pontides, northeastern Turkey. Bull Geol Soc Am 131:1889–1906

Karslı O, Şengün F, Dokuz A, Kandemir R, Aydin F, Andersen T (2020) Silurian to Early Devonian arc magmatism in the western Sakarya Zone (NWTurkey), with inference to the closure of the Rheic Ocean. Lithos 370–371:105641

Kaygusuz A, Arslan M, Siebel W, Sipahi F, İlbeyli N (2012) Geochronological evidence and tectonic significance of Carboniferousmagmatismin the southwest Trabzon area, eastern Pontides, Turkey. Int Geol Rev 54:1776–1800

Kaygusuz A, Arslan M, Sipahi F, Temizel İ (2016) U-Pb zircon chronology and petrogenesis of Carboniferous plutons in the northern part of the Eastern Pontides, NE Turkey: Constraints for Paleozoic magmatism and geodynamic evolution. Gond Res 39:327–346

Konak N, Alan İ, Bakırhan B, Bedi Y, Dönmez M, Pehlivan Ş, Sevin M, Türkecan A, Yusufoğlu H (2016) Geological map of Turkey 1:1 000 000 scale, one sheet, Maden Tetkik ve Arama Genel Müdürlüğü Ankara

Konuk YT (1977) About the age of the Bornova Flysch (in Turkish). Ege Üniversitesi Fen Fakültesi Dergisi, Seri B 1:65–73

Koralay OE, Satır M, Dora OÖ (2001) Geochemical and geochronological evidence for Early Triassic calc-alkaline magmatism in the Menderes Massif, western Turkey. Int J Earth Sc 89:822–835

Koralay OE, Candan O, Akal C, Dora OÖ, Chen F, Satır M, Oberhansli R (2011) The geology and geochronology of the Pan-African and Triassic metagranitoids in the Menderes Massif, Western Anatolia, Turkey. Bull Mineral Res Explor 142:69–119

Kozur H (1998) The age of the siliciclastic series ("Karareis formation") of the western Karaburun peninsula, western Turkey. Paleontol Polonica 58:172–187

Kylander-Clark ARC, Hacker BR, Cottle JM (2013) Laser-ablation split-stream ICP petrochronology. Chem Geol 345:99–112

Lagos M, Scherer EE, Tomaschek F, Münker C, Keiter M, Berndt J, Ballhaus C (2007) High precision Lu–Hf geochronology of Eocene eclogite-facies rocks from Syros Cyclades Greece. Chem Geol 243:16–35

Liu Z, Zhu DC, Jagoutz O, Rezeau H, Wang Q, Eyuboglu Y (2021) Magmatic evolution following damp tholeiitic and wet calc-alkaline liquid lines of descent: an Eastern Pontides (NE Turkey) example. J Petrol. https://doi.org/10.1093/petrology/egaa088

Loos S, Reischmann T (1999) The evolution of the southern Menderes Massif in SW Turkey as revealed by zircon dating. J Geol Soc London 156:1021–1030

Löwen K, Meinhold G, Güngör T, Berndt J (2017) Palaeotethys-related sediments of the Karaburun Peninsula western Turkey: constraints on provenance and stratigraphy from detrital zircon geochronology. Int J Earth Sci 106:2771–2796

Masse JP, Işıntek İ (2000) Algues dasycladales de l'Albien de la Peninsule de Karaburun- Turquie. Rev Micropaleontol 43:365–380

Meinhold G, Reischmann T, Kostopoulos D, Lehnert O, Matukov D, Sergeev S (2008) Provenance of sediments during subduction of Palaeotethys: detrital zircon ages and olistolith analysis in Palaeozoic sediments from Chios Island, Greece. Palaeo Palaeo Palaeo 263:71–91

Moghadam HS, Li XH, Ling XX, Stern RJ, Santos JF, Meinhold G, Ghorbani G, Shahab S (2015) Petrogenesis and tectonic implications of Late Carboniferous A-type granites and gabbro-norites in

NW Iran: geochronological and geochemical constraints. Lithos 212:266–279
Moix P, Beccaletto L, Kozur HW, Hochard C, Rosselet F, Stampfli GM (2008) A new classification of the Turkish terranes and sutures and its implication for the paleotectonic history of the region. Tectonophysics 451:7–39
Mueller MA, Licht A, Campbell C, Ocakoğlu F, Akşit GG, Métais G, Coster PMC, Beard KC, Taylor MH (2022) Sedimentary provenance from the evolving forearc-to-foreland Central Sakarya Basin western Anatolia reveals multi-phase intercontinental collision. Geo Geo Geo 23:e2021GC010232
Ocakoğlu F, Hakyemez A, Açıkalın S, ÖzkanAltıner S, Büyükmeriç Y, Licht A, Demircan H, Şafak Ü, Yıldız A, Yilmaz IÖ, Wagreich M, Campbell C (2019) Chronology of subduction and collision along the İzmir-Ankara suture in Western Anatolia: records from the Central Sakarya Basin. Int Geol Rev 61:1244–1269
Okay AI (2008) Geology of Turkey: A synopsis. Anschnitt Zeitschrift für Kunst und Kultur im Bergbau Beiheft 21:19–42 (**Veröffentlichungen aus dem Deutschen Bergbau-Museum Bochum Nr 157**)
Okay AI, Altıner D (2007) A condensed Mesozoic section in the Bornova Flysch Zone: A fragment of the Anatolide-Tauride carbonate platform. Turk J Earth Sc 16:257–279
Okay AI, Altıner D (2016) Carbonate sedimentation in an active margin: Cretaceous history of the Haymana region Pontides. Int J Earth Sci 105:2013–2030
Okay AI, Göncüoğlu MC (2004) Karakaya Complex: a review of data and concepts. Turk J Earth Sc 13:77–95
Okay AI, Nikishin AM (2015) Tectonic evolution of the southern margin of Laurasia in the Black Sea region. Int Geol Rev 57:1051–1076
Okay AI, Tüysüz O (1999) Tethyan sutures of northern Turkey. Geol Soc London Sp Publ 156:475–515
Okay AI, Whitney DL (2010) Blueschists eclogites ophiolites and suture zones in northwest Turkey: a review and a field excursion guide. Ofioliti 35:131–172
Okay AI, Şengör AMC, Görür N (1994) Kinematic history of the opening of the Black Sea and its effect on the surrounding regions. Geology 22:267–270
Okay AI, Satır M, Tüysüz O, Akyüz S, Chen F (2001) The tectonics of the Strandja Massif: Variscan and mid-Mesozoic deformation and metamorphism in the northern Aegean. Int J Earth Sci 90:217–233
Okay AI, Satır M, Siebel W (2006) Pre-Alpide orogenic events in the Eastern Mediterranean region. Geol Soc London Memoirs 32:389–405
Okay AI, Satır M, Shang CK (2008) Ordovician metagranitoid from the Anatolide-Tauride Block northwest Turkey -geodynamic implications. Terra Nova 20:280–288
Okay AI, Işıntek İ, Altıner D, Özkan-Altıner S, Okay N (2012) An olistostrome- mélange belt formed along a major suture: Bornova Flysch Zone western Turkey. Tectonophysics 568–569:282–295
Okay AI, Sunal G, Sherlock S, Altıner D, Tüysüz O, Kylander-Clark ARC, Aygül M (2013) Early Cretaceous sedimentation and orogeny on the active margin of Eurasia: southern Central Pontides, Turkey. Tectonics 32:1247–1271
Okay AI, Sunal G, Tüysüz O, Sherlock S, Keskin M, Kylander-Clark ARC (2014) Low-pressure - high-temperature metamorphism during extension in a Jurassic magmatic arc Central Pontides Turkey. J Metamorp Geol 32:49–69
Okay AI, Altıner D, Sunal G, Tüysüz O, Aygül M, Akdoğan R, Altıner S, Simmons M (2018) Geological Evolution of the Central Pontides. Geol Soc London Sp Publ 464:33–67
Okay AI, Altıner D, Kylander-Clark ARC (2019) Major Late Cretaceous mass flows in central Turkey recording the disruption of the Mesozoic continental margin. Tectonics 38:960–989
Okay AI, Sunal G, Sherlock S, Kylander-Clark ARC, Özcan E (2020) İzmir-Ankara suture as a Triassic to Cretaceous plate boundary—Data from central Anatolia. Tectonics 38:e2019TC005849
Okay AI, Altıner D, Danelian T, Topuz G, Özcan E, Kylander-Clark AR (2022) Subduction-accretion complex with boninitic ophiolite slices and Triassic limestone seamounts: Ankara Mélange central Anatolia. Geological Magazine 159(10):1699–1726. https://doi.org/10.1017/S0016756822000504
Okay AI, Siyako M (1993) The new position of the Izmir-Ankara Neo-Tethyan suture between İzmir and Balıkesir (in Turkish). In: Turgut S (ed) Tectonics and Hydrocarbon Potential of Anatolia and Surrounding Regions Proceedings of the Ozan Sungurlu Symposium 333–355
Özbey Z, Ustaomer T, Robertson AHF, Ustaömer PA (2013) Tectonic significance of Late Ordovician granitic magmatism and clastic sedimentation on the northern margin of Gondwana (Tavsanli Zone NW Turkey). J Geol Soc 70:159–173
Özdamar Ş, Billor MZ, Sunal G, Esenli F, Roden MF (2013) First U-Pb SHRIMP zircon and 40Ar/39Ar ages of metarhyolites from the Afyon-Bolkardag Zone SW Turkey: Implications for the rifting and closure of the Neo-Tethys. Gond Res 24:377–391
Özer S, İrtem O (1982) Geological setting stratigraphy and facies of the Upper Cretaceous limestones in the Işıklar-Altındağ (Bornova- İzmir) area (in Turkish). Türkiye Jeoloji Kurumu Bülteni 25:41–47
Özgül N (1976) Some principal geological features of the Taurides (in Turkish). Türkiye Jeoloji Kurumu Bülteni 19:65–78
Özgül N (2012) Stratigraphy and some structural features of the Istanbul Palaeozoic. Turk J Earth Sci 21:817–866
Parlak O, Karaoğlan F, Rızaoğlu T, Klötzli U, Koller F, Billo Z (2013) U-Pb and 40Ar/39Ar geochronology of the ophiolites and granitoids from the Tauride belt: Implications for the evolution of the inner tauride suture. J Geodyn 65:22–37
Plunder A, Agard P, Chopin C, Pourteau A, Okay AI (2015) Accretion underplating and exhumation along a subduction interface: From subduction initiation to continental subduction (Tavşanlı zone W Turkey). Lithos 226:233–254
Poisson A, Şahinci A (1988) La série mésozoïque de Kemalpaşa et le flysch paléocene d'İzmir au Nord-Ouest du Menderes (Anatolie occidentale Turquie): Un jalon du microcontinent taurique. CR Acad Sci Paris 307:1075–1080
Pourteau A, Sudo M, Candan O, Lanari P, Vidal O, Oberhänsli R (2013) Neotethys closure history of Anatolia: insights from 40Ar–39Ar geochronology and P-T estimation in high-pressure metasedimentary rocks. J Metamorph Geol 31:585–606
Robertson AHF, Dixon JD (1984) Introduction: aspects of the Geological Evolution of the Eastern Mediterranean. Geol Soc London Sp Publ 17:1–74
Robertson AHF, Pickett EA (2000) Palaeozoic-Early Tertiary Tethyan evolution of mélanges rift and passive margin units in the Karaburun Peninsula (western Turkey) and Chios island (Greece). Geol Soc London Sp Publ 173:43–82
Robertson AHF, Ustaömer T (2009) Upper Palaeozoic subduction/accretion processes in the closure of Palaeotethys: Evidence from the Chios Melange (E Greece), the Karaburun Melange (W Turkey) and the Teke Dere Unit (SW Turkey). Sed Geol 220:29–59
Robertson AHF, Parlak O, Ustaömer T (2009) Melange genesis and ophiolite emplacement related to subduction of the northern margin of the Tauride-Anatolide continent, central and western Turkey. Geol Soc London Sp Publ 311:9–66
Robertson AHF, Parlak O, Ustaömer TO (2013) Late Palalaeozoic-Early Cenozoic tectonic development of Southern Turkey and the easternmost Mediterranean region: evidence from the interrelations of continental and oceanic units. Geol Soc London Sp Publ 372:9–48

Robertson AHF, Parlak O, Ustaömer T, Taslı K, Dumitrica P (2021) Late Palaeozoic-Neogene sedimentary and tectonic development of the Tauride continent and adjacent Tethyan ocean basins in eastern Turkey: New data and integrated interpretation. J Asian Earth Sci 220:104859

Sałacinska A, Gerdjikov I, Kounov A, Chew D, Szopa K, Gumsley A, Kocjan I, Marciniak-Maliszewska B, Drakou F (2022) Variscan magmatic evolution of the Strandja Zone (Southeast Bulgaria and northwest Turkey) and its relationship to other north Gondwanan margin terranes. Gond Res 109:253–273

Saner S (1980) Paleogeographic interpretation of the Jurassic and younger sedimentation in the Mudurnu-Göynük basin (in Turkish). Türkiye Jeoloji Kurumu Bülteni 23:39–52

Sarı B (2013) Late Maastrichtian-Late Palaeocene planktic foraminiferal biostratigraphy of the matrix of the Bornova Flysch Zone around Bornova (İzmir, Western Anatolia, Turkey). Turkish J Earth Sci 22:143–171

Schmidt A, Pourteau A, Candan O, Oberhänsli R (2015) Lu–Hf geochronology on cm-sized garnets using microsampling: New constraints on garnet growth rates and duration of metamorphism during continental collision (Menderes Massif Turkey). Earth Planet Sci Lett 432:24–35

Şengör AMC, Yılmaz Y (1981) Tethyan evolution of Turkey a plate tectonic approach. Tectonophysics 75:181–241

Sherlock S, Kelley SP, Inger S, Harris N, Okay AI (1999) 40Ar-39Ar and Rb-Sr geochronology of high-pressure metamorphism and exhumation history of the Tavsanli Zone NW Turkey. Contrib Min Pet 137:46–58

Solak C, Taslı K, Sarı B (2015) Stratigraphy and depositional history of the Cretaceous carbonate successions in the Spil Mountain (Manisa, W Turkey). Cretaceous Res 53:1–18

Sunal G, Natal'in B, Satır M, Toraman E (2006) Paleozoic magmatic events in the Strandja Masif, NW Turkey. Geodin Acta 19:283–300

Sunal G, Satır M, Natal'in B, Topuz G, von der Scmidt O (2011) Metamorphism and diachronous cooling in a contractional orogen: the Strandja Massif NW Turkey. Geol Mag 148:580–596

Sunal G, Akın A, Erturaç MK, Ay C, Dunkl I (2022) Paleo-exhumation histories of the Sakarya and the Istanbul Zones of the Western Pontides, the Almacık Block and its surroundings NW Turkey. Int Geol Rev. https://doi.org/10.1080/00206814.2022.2084645

Tekin UK, Göncüoğlu MC (2007) Discovery of the oldest (Upper Ladinian to Middle Carnian) radiolarian assemblages from the Bornova Flysch Zone in western Turkey: Implications for the evolution of the Neotethyan Izmir-Ankara ocean. Ofioliti 32:131–150

Tekin UK, Göncüoğlu CM, Uzunçimen S (2012) Radiolarian assemblages of Middle and Late Jurassic to early Late Cretaceous (Cenomanian) ages from an olistolith record pelagic deposition within the Bornova Flysch Zone in western Turkey. Bull Soc Géol France 183:307–318

Topuz G, Altherr R, Siebel W, Schwartz WH, Zack T, Hasözbek A, Barth B, Satır M, Şen C (2010) Carboniferous high-potassium I-type granitoid magmatism in the Eastern Pontides: The Gümüşhane pluton (NE Turkey). Lithos 116:92–110

Topuz G, Candan O, Okay AI, von Quadt A, Othman M, Zack T, Wang J (2020) Silurian anorogenic basic and acidic magmatism in northwest Turkey: Implications for the opening of the Paleo-Tethys. Lithos, 356–357, article 105302

Ünalan G, Yüksel V, Tekeli T, Gönenç O, Seyirt Z, Selahi H (1976) Upper Cretaceous – Lower Tertiary stratigraphy and paleogeographic evolution of the Haymana-Polatlı region (southwest Ankara) (in Turkish). Türkiye Jeoloji Kurumu Bülteni 19:159–176

Ustaomer PA, Mundil R, Renne PR (2005) U/Pb and Pb/Pb zircon ages for arc-related intrusions of the Bolu Massif (W Pontides, NW Turkey): evidence for Late Precambrian (Cadomian) age. Terra Nova 17:215–223

Ustaomer PA, Ustaomer T, Robertson AHF (2012) Ion probe U-Pb dating of the Central Sakarya basement: A peri-Gondwana terrane intruded by late Lower Carboniferous subduction/collision-related granitic rocks. Turk J Earth Sci 21:905–932

Ustaömer T, Robertson AHF, Ustaömer PA, Gerdes A, Peytcheva I (2016) Implications of U–Pb and Lu–Hf isotopic analysis of detrital zircons for the depositional age provenance and tectonic setting of the Permian–Triassic Palaeotethyan Karakaya Complex NW Turkey. Int J Earth Sci 105:7–38. https://doi.org/10.1007/s00531-015-1225-8

Ustaömer T, Ustaömer PA, Robertson AHF, Gerdes A (2020) U-Pb-Hf isotopic data from detrital zircons in late Carboniferous and Mid-Late Triassic sandstones and also Carboniferous granites from the Tauride and Anatolide continental units in S Turkey: implications for Tethyan palaeogeography. Inter Geol Rev 62:1159–1186

van Hinsbergen DJJ, Torsvik TH, Schmid SM, Matenco LC, Maffione M, Vissers RLM, Gürer D, Spakman W (2020) Orogenic architecture of the Mediterranean region and kinematic reconstruction of its tectonic evolution since the Triassic. Gond Res 81:79–229

Xin G-Y, Chu Y, Su B-X, Lin W, Cui M-M, Liu X, Uysal I, Li J-L, Feng Z-T (2022) Subduction initiation in the Neo-Tethys and formation of the Bursa ophiolite in NW Turkey. Lithos. https://doi.org/10.1016/jlithos2022106746

Yılmaz İ, YılmazŞahin Ş, Aysal N, Güngör Y, Akgündüz A, Bayhan UC (2021) Geochronology, geochemistry and tectonic setting of the Cadomian (Ediacaran–Cambrian) magmatism in the Istranca (Strandja) Massif: new insights into magmatism along the northern margin of Gondwana in NW Turkey. Int Geol Rev. https://doi.org/10.1080/00206814.2021.1901249

YılmazŞahin S, Aysal N, Güngör Y, Peytcheva I, Neubauer F (2014) Geochemistry and U-Pb zircon geochronology of metagranites in Istranca (Strandja) Zone NW Pontides Turkey: Implications for the geodynamic evolution of Cadomian orogeny. Gond Res 26:755–771

Zanchi A, Garzanti E, Larghi C, Angiolini L, Gaetani M (2003) The Variscan orogeny in Chios (Greece): Carboniferous accretion along a Palaeotethyan active margin. Terra Nova 15:213–223

Zlatkin O, Avigad D, Gerdes A (2013) Evolution and provenance of Neoproterozoic basement and Lower Paleozoic siliciclastic cover of the Menderes Massif (Western Taurides): Coupled U-Pb–Hf zircon isotope geochemistry. Gond Res 23:682–700